C. R. Mecanique 345 (2017) 844–867

Contents lists available at ScienceDirect

Comptes Rendus Mecanique

www.sciencedirect.com

Stochastic model reduction for robust dynamical characterization of structures with random parameters

Martin Ghienne, Claude Blanzé, Luc Laurent *

Laboratoire de mécanique des structures et des systèmes couplés, Conservatoire national des arts et métiers, case courrier 2D6R10, 2, rue Conté, 75003 Paris, France [1]

ARTICLE INFO

Article history:
Received 25 July 2017
Accepted 18 September 2017
Available online 6 October 2017

Keywords:
Random eigenvalue problems
Statistical distributions
Linear stochastic systems
Perturbation
Simplified resolution method
Proximity factor

ABSTRACT

In this paper, we characterize random eigenspaces with a non-intrusive method based on the decoupling of random eigenvalues from their corresponding random eigenvectors. This method allows us to estimate the first statistical moments of the random eigenvalues of the system with a reduced number of deterministic finite element computations. The originality of this work is to adapt the method used to estimate each random eigenvalue depending on a global accuracy requirement. This allows us to ensure a minimal computational cost. The stochastic model of the structure is thus reduced by exploiting specific properties of random eigenvectors associated with the random eigenfrequencies being sought. An indicator with no additional computation cost is proposed to identify when the method needs to be enhanced. Finally, a simple three-beam frame and an industrial structure illustrate the proposed approach.

© 2017 Académie des sciences. Published by Elsevier Masson SAS. This is an open access article under the CC BY-NC-ND license (http://creativecommons.org/licenses/by-nc-nd/4.0/).

1. Introduction

Requirements on system performance are increasingly stringent, which leads us to question the design rules currently used in structural engineering. The use of safety factors that are often inconsistent and confusing is no longer sufficient in many leading-edge fields, and it is necessary to decrease the gap between the observed behavior of a structure and predictions from numerical simulations based on deterministic models. In order to accurately predict the real behavior of a structure, the variability of the observed behavior needs to be modeled. This variability is mainly due to the system parameter's randomness. The probabilistic approach is adapted to numerical resolution [1,2]. This is thus the framework adopted for this work.

The aim is to robustly characterize the vibrational response of a structure in a random manner from a finite element model of the structure. We are particularly looking for the eigenspace characterization of linear systems with dynamic properties considered as random variables. Methods based on statistical sampling provide a good framework to solve the random dynamic problem; nevertheless, they need intensive computation to remain accurate [3,4]. The performance of this kind of method strongly depends on the quality of the random number generator and the total computational cost increases dramatically with the cost of one deterministic case. For these reasons, reduced-order models in a context such as PGD [5], for instance, or non-sampling methods have been introduced. Along the latter, different techniques have been developed over

* Corresponding author.
E-mail addresses: martin.ghienne@lecnam.net (M. Ghienne), claude.blanze@lecnam.net (C. Blanzé), luc.laurent@lecnam.net (L. Laurent).
[1] www.lmssc.cnam.fr

https://doi.org/10.1016/j.crme.2017.09.006
1631-0721/© 2017 Académie des sciences. Published by Elsevier Masson SAS. This is an open access article under the CC BY-NC-ND license (http://creativecommons.org/licenses/by-nc-nd/4.0/).

the last few decades. Two particular approaches are mainly used in the literature to approximate the statistical properties of the response of a random system: the perturbation and the spectral methods.

The perturbation method is based on an approximation of the random variable of interest through the truncation of its Taylor expansion. Its implementation is pretty easy, but as high-order perturbation terms are computationally intensive, the expansion is generally limited to the second order. Moreover, variations of the system parameters should remain small to guarantee the accurate estimation of statistical moments [6]. Generally, random variables are expanded by their Taylor series about their mean value. For example, Collins and Thomson [7] estimate statistics of random eigenvalues and eigenvectors. Adhikari and Friswell [8] propose to expand around an optimal point in order to better approximate the first moments of random eigenvalues. Nair and Keane [9] use a perturbation method to define an approximation subspace and to estimate the system's random eigenvectors.

The Spectral Stochastic Finite Element Method (SSFEM) was introduced by Ghanem and Spanos in [10], inspired by Wiener's works [11]. The method is based on a discretization of the random variables of interest among a finite random space. The random variables are decomposed on the basis of orthogonal polynomials in terms of the multi-dimensional random variable with a specific probability distribution. This basis is called the polynomial chaos. For problems with Gaussian random input parameters, the best-suited basis consists of a set of multidimensional Hermite polynomials [12]; it ensures fast convergence and accurate approximation of the random variables. If the input parameters are not Gaussian, other proper bases have been developed to ensure an optimal convergence [13]. Once the decomposition basis is chosen, the coefficients of the decomposed random variable need to be computed. For this purpose, a Galerkin-based method described in [14] allows us to estimate the coefficients using Monte Carlo sampling. This method suffers from its sensibility to the quality of the random number generator [15,16] and becomes quickly computationally intensive in the case of high-order polynomials or of a high number of random parameters. To overcome these drawbacks, Ghanem and Ghosh [14] propose another Galerkin-based method for reducing the problem to a set of deterministic non-linear equations.

In order to characterize the eigenspace of a system with random dynamic properties, polynomial chaos methods give a general and accurate framework, but their implementation is rather complex. On the other hand, perturbation methods are easy to implement, but their intrinsic assumptions limit their application to academic problems or small variations of the input parameters. Based on these techniques, Pascual and Adhikari [17] have proposed and compared methods hybridizing perturbation approach and polynomial chaos expansion applied to eigenvalue problems.

The aim of this paper is to propose a non-intrusive approach to characterize a random eigenspace with a reduced number of deterministic finite element computations. A simple observation is at the origin of the proposed approach: in some cases, the eigenvalues of a structure with random parameters are random, but the corresponding eigenvectors are quite deterministic. In these cases, a simple deterministic computation is sufficient to characterize the random eigenmode. For the remaining eigenvalues, it is then necessary to use more accurate methods. This approach, referred to as the SMR method for Stochastic Model Reduction approach, consists in adapting stochastic modeling to each random eigenvalue depending on the global accuracy requirements on the whole set of random eigenvalues. Finally, the proposed approach minimizes the computational cost by concentrating computational resources on particular eigendata sets according to their configuration. The next section describes the SMR approach and its different refinement levels. As the proposed approach relies on the random eigenfrequencies configuration, an appropriate indicator referred to as the "proximity factor" is also developed in this section. Then a three-degrees-of-freedom test case illustrates the accuracy of the method, depending on the random eigenfrequencies configuration. We characterize the indicator for a large number of configurations. In the fourth section, the approach is applied to a more realistic system consisting of a frame with different random Young's moduli. Finally, an industrial structure is used to illustrate the efficiency of the SMR approach in terms of computation time and accuracy of statistical moments estimation.

2. Stochastic model reduction

2.1. Problem presentation

The general eigenvalue problem of undamped or proportionally damped systems can be expressed for a problem with n_d degrees of freedom by

$$\lambda_k(\theta)\mathbf{M}(\theta)\boldsymbol{\Phi}_k(\theta) = \mathbf{K}(\theta)\boldsymbol{\Phi}_k(\theta) \tag{1}$$

where

$$\lambda_k(\theta) \in \mathbb{R}, \quad \boldsymbol{\Phi}_k(\theta) \in \mathbb{R}^{n_d}, \quad \mathbf{M}(\theta) \in \mathbb{R}^{n_d \times n_d}, \quad \mathbf{K}(\theta) \in \mathbb{R}^{n_d \times n_d}, \quad \theta \in \Omega$$

λ_k and $\boldsymbol{\Phi}_k$ are the kth eigenvalue and the kth associated eigenvector. The relationship between the eigenvalues and the natural frequencies of the system is $\lambda_k = \omega_k^2$. The eigenvector $\boldsymbol{\Phi}_k$ is assumed to be mass normalized so that $\boldsymbol{\Phi}_k^\top \mathbf{M} \boldsymbol{\Phi}_k = 1$. $(\Omega, \mathcal{F}, p)$ is the abstract probability space associated with the underlying physical experiments. $\theta \in \Omega$ is a basic event from the complete probability space Ω. The space of square integrable random variables is denoted by $L_2(\Omega)$ and forms a Hilbert space with the norm $\|\cdot\|_{L_2(\Omega)}$. Matrices $\mathbf{M}(\theta)$ and $\mathbf{K}(\theta)$ represent the mass and stiffness matrices of the structure. Their randomness is due to the physical parameters of the structure such as mass density, Young's modulus or geometric

properties. In this paper, E[·], Var[·] and $\sigma[\cdot]$ denote respectively the mathematical expectation, variance, and standard deviation.

To facilitate the understanding of the upcoming developments, we consider the case of a structure composed of n sub-structures with n different Young's moduli $(Y_1, Y_2, ..., Y_n)$, for example, a metallic structure provided with piezoelectric patches. The Young's moduli are assumed to be the only random parameters in the considered problem. Thus the stiffness matrix $\mathbf{K}(\theta)$ is a random matrix and $\mathbf{M}$ remains deterministic. The global stiffness matrix can be written according to different stiffness matrices relating to each sub-structure:

$$\mathbf{K}(\theta) = \sum_{i=1}^{n} \mathbf{K}_i(\theta) = \sum_{i=1}^{n} \gamma_i(\theta)\mathbf{K}_i \tag{2}$$

where $\gamma_i(\theta)$ is the random parameter corresponding to the ith Young's modulus and defined as:

$$\gamma_i(\theta) = \frac{Y_i(\theta)}{Y_{0i}}; \quad Y_{0i} = \mathrm{E}[Y_i(\theta)] \quad \text{and} \quad \mathrm{E}[\gamma_i(\theta)] = 1$$

$\mathbf{K}_i$ are the sensitivity stiffness matrices of the global stochastic stiffness matrix $\mathbf{K}(\theta)$ with respect to the parameter $\gamma_i(\theta)$. With this notation, the stochastic behavior is only taken into account by the coefficient $\gamma_i(\theta)$. These $\mathbb{R}^{n_d \times n_d}$ matrices correspond, in this linear case, to a global sub-structure stiffness matrix obtained with the mean value of the Young modulus (stiffness matrix of the sub-structure reshaped in the whole basis of degrees of freedom of the considered problem). In addition, $\mathbf{K}_i(\theta)$ are the global sub-structure stochastic stiffness matrices.

The proposed approach relies on the observation that, considering a structure with random parameters and a set of random eigenvalues to be determined, some eigenvectors associated with a particular eigenvalue only vary slightly with respect to the input random parameters, and therefore could be considered as deterministic as a first approximation. It is then extremely cheap (in computational terms) to estimate the corresponding random eigenvalues. The available computational resources could be concentrated in more accurate methods to estimate the remaining random eigenvalues of the set of interest. When the eigenvector can not be considered as deterministic, we propose to expand it as a function of the input random parameters. It allows us to take into account the variability of the random eigenvector and then to deduce the corresponding random eigenvalue. With this approach, the randomness of the kth eigenmode $(\lambda_k(\theta), \Phi_k(\theta))$ is reduced depending on the eigenmode configuration. This approach is referred to as SMR for Stochastic Model Reduction. The approach has at least two refinement levels that we refer to hereafter as SMR1 and SMR2.

2.2. The Stochastic Model Reduction approach

This subsection illustrates the basic assumptions of the SMR approach [18,19]. First, we present the first refinement level of the SMR approach. The determination of a particular couple eigenvalue–eigenvector is based on the assumption that the eigenvector does not vary with the random input parameters. The foundation of this refinement level is then illustrated with two different points of view. Then the SMR second refinement level is presented. It is based on the expansion of the eigenvector as a function of the input random parameters to take into account its variability and improve the random eigenvalue model. A method to compute the eigenvector derivatives, adapted to the SMR framework, is then proposed. Finally the SMR resolution approach is summarized, and a criterion is proposed to identify when the first or the second refinement level should be used.

2.2.1. First refinement level: SMR1

According to the first assumption of the SMR approach, it is assumed that Young's moduli variations around an expected value do not change the eigenvector shapes of the structure. Therefore, the matrix of random eigenvectors corresponds to the matrix of eigenvectors calculated with the expected value parameters:

$$\mathbf{\Phi}(\theta) = \overline{\mathbf{\Phi}} \tag{3}$$

This assumption, added to the mass normalization of eigenvectors $\mathbf{\Phi}_k$, allows us to rewrite the kth random frequency as:

$$\lambda_k(\theta) = \omega_k^2(\theta) = \sum_{i=1}^{n} \gamma_i(\theta)\overline{\mathbf{\Phi}_k}^{\top}\mathbf{K}_i\overline{\mathbf{\Phi}_k} = \sum_{i=1}^{n} \lambda_{ki}\gamma_i(\theta) \tag{4}$$

where

$$\lambda_{ki} = \overline{\mathbf{\Phi}_k}^{\top}\mathbf{K}_i\overline{\mathbf{\Phi}_k} \tag{5}$$

The coefficients of this expansion are deterministic. The randomness of the eigenvalue is only due to the input random parameters. This simplification could be used, for example, in the case of a structure composed of two sub-structures of different sizes. The variation of Young's modulus of the smallest sub-structure around its expected value will have a negligible effect on the main structure.

2.2.2. First central moments

The main advantage of this first refinement level is to obtain the closed form of the approximate eigenvalue. Therefore, the two first central moments of the random eigenvalues are obtained with no computational cost. Indeed, assuming that the n Young moduli $(Y_i)_{1\leq i\leq n}$ are independent random variables, the expected value of the kth eigenvalue is obtained directly:

$$E[\lambda_k] = \sum_{i=1}^{n} E[\gamma_i]\boldsymbol{\Phi}_k^{\top}\mathbf{K}_i\boldsymbol{\Phi}_k = \sum_{i=1}^{n} \boldsymbol{\Phi}_k^{\top}\mathbf{K}_i\boldsymbol{\Phi}_k = \sum_{i=1}^{n} \lambda_{ki} = \overline{\lambda}_k \tag{6}$$

where $\overline{\lambda}_k$ represents the deterministic eigenvalue associated with the deterministic eigenvalue problem:

$$\mathbf{K}_0\boldsymbol{\Phi}_k = \overline{\lambda}_k\mathbf{M}\boldsymbol{\Phi}_k \tag{7}$$

and

$$\mathbf{K}_0 = \mathbf{K}|_{\gamma_i(\theta)=1} = \sum_{i=1}^{n}\mathbf{K}_i \tag{8}$$

The variance of the kth eigenvalue is:

$$\mathrm{Var}[\lambda_k] = \sum_{i=1}^{n}\lambda_{ki}^2\,\mathrm{Var}[\gamma_i] = \sum_{i=1}^{n}\lambda_{ki}^2\delta_i^2 \tag{9}$$

where $\delta_i = \sigma[Y_i]/\mathrm{E}[Y_i]$ is the coefficient of variation of the random parameter Y_i.

It can be noticed that the estimation of the two first statistical moments is obtained with only one deterministic finite element computation and the knowledge of the first moment of the input random parameters. In fact, there is no need for stochastic computation.

2.2.3. Two illustrations of the SMR first assumption

First order Taylor expansion. The first assumption of the SMR approach could be illustrated considering a first-order Taylor expansion of the kth random eigenvalue $\lambda_k(\boldsymbol{\gamma}(\theta))$ about the mean of $\mathrm{E}[\boldsymbol{\gamma}(\theta)] = \boldsymbol{\gamma}_0$. This approach corresponds to the perturbation method largely covered in the literature [6,8]. Recall that $\boldsymbol{\gamma}(\theta)$ is the random vector representing the n input parameters of the vibrational system. For convenience, the randomness dependency of $\boldsymbol{\gamma}(\theta)$ will be implicit in this section, and we will use the following notation $\boldsymbol{\gamma}$.

$$\lambda_k(\boldsymbol{\gamma}) = \lambda_k(\boldsymbol{\gamma}_0) + \sum_{i=1}^{n}\left(\left.\frac{\partial\lambda_k}{\partial\gamma_i}\right|_{\boldsymbol{\gamma}=\boldsymbol{\gamma}_0}(\gamma_i-\gamma_{i0})\right) \tag{10}$$

As developed by Fox and Kapoor [20], the expression of the rate of change of an eigenvalue is:

$$\frac{\partial\lambda_k}{\partial\gamma_i}(\boldsymbol{\gamma}) = \boldsymbol{\Phi}_k^{\top}(\boldsymbol{\gamma})\left[\frac{\partial\mathbf{K}}{\partial\gamma_i}(\boldsymbol{\gamma}) - \lambda_k(\boldsymbol{\gamma})\frac{\partial\mathbf{M}}{\partial\gamma_i}(\boldsymbol{\gamma})\right]\boldsymbol{\Phi}_k(\boldsymbol{\gamma}) \tag{11}$$

Assuming that $\boldsymbol{\Phi}_k$ is mass-normalized so that $\boldsymbol{\Phi}_k^{\top}\mathbf{M}\boldsymbol{\Phi}_k = 1$, the first term of the Taylor expansion is $\lambda_k(\boldsymbol{\gamma}_0) = \overline{\boldsymbol{\Phi}_k}^{\top}\mathbf{K}\overline{\boldsymbol{\Phi}_k}$. The kth random eigenvalue can be expressed using the expression of the eigenvalue derivative at $\boldsymbol{\gamma} = \boldsymbol{\gamma}_0$:

$$\lambda_k(\boldsymbol{\gamma}) = \overline{\boldsymbol{\Phi}_k}^{\top}\mathbf{K}\overline{\boldsymbol{\Phi}_k} + \sum_{i=1}^{n}\left[\left(\overline{\boldsymbol{\Phi}_k}^{\top}\left[\frac{\partial\mathbf{K}}{\partial\gamma_i}(\boldsymbol{\gamma}_0) - \overline{\lambda}_k\frac{\partial\mathbf{M}}{\partial\gamma_i}(\boldsymbol{\gamma}_0)\right]\overline{\boldsymbol{\Phi}_k}\right)(\gamma_i-\gamma_{i0})\right] \tag{12}$$

It is then obvious that the random eigenvalue at first order depends only on the corresponding deterministic eigenvector.

Parametric approach. The basic assumption can be addressed with a parametric approach of the eigenvalue problem. The behavior of eigenvalues associated with a change of parameters is a problem intensively studied in the literature [21–23]. Systems with parameters varying over a large range often undergo frequency coalescence and/or veering. This phenomenon appears when two eigenvalue loci approach each other closely and suddenly veer away again, each one taking on the trajectory of the other. The eigenvectors corresponding to each one of the two modes swap as the loci pass through the veering area. Outside this area, the eigenvectors remain constant. This phenomenon is illustrated in Fig. 1. This figure presents the eigenvalue loci (a) of a simple three-degrees-of-freedom (DoF) undamped spring-mass system (b). The parameters of this system are tuned to observe the veering effect between the second and the third eigenvalues when the stiffness k_2 is varying. Other stiffness parameters are $k_i = [1, k_2, 3, 0.1, 0.1, 0.1]$, and the three masses are $m_1 = m_2 = m_3 = 1$. The windows over each eigenvalue locus represent the corresponding eigenvector for this k_2 range of values.

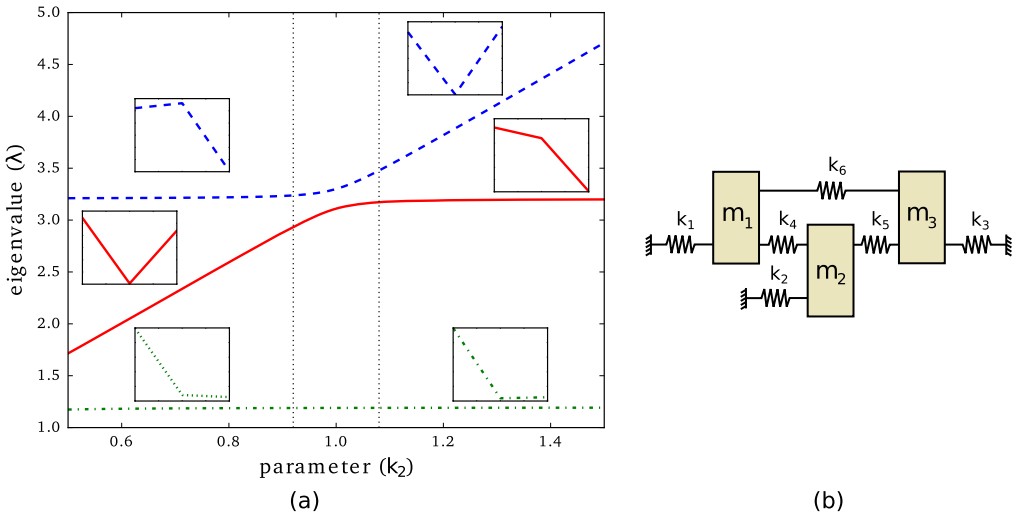

Fig. 1. Eigenvalue loci with the corresponding eigenvector (a) of a 3 DoF system (b).

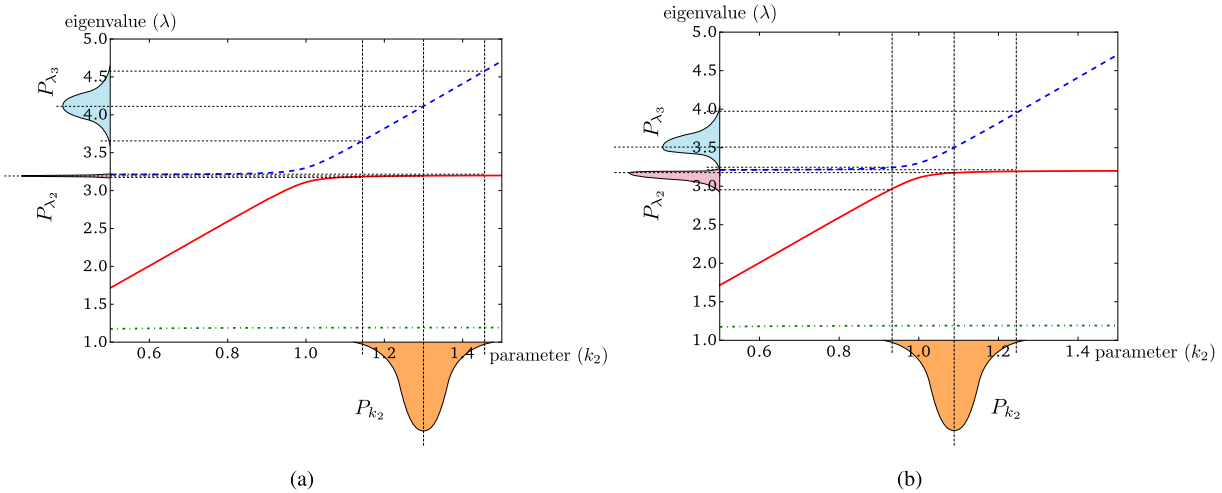

Fig. 2. Marginal density functions of the second and third eigenvalues of a three DoF system when the *pdf* of the input parameter is out of the veering area (a) or cross it (b).

Let us consider the case of a system with a single parameter $p(\theta)$ randomly varying with a given probability density function (*pdf*). The variability of this parameter could be compared to the eigenvalue loci of the system. Two particular cases could be highlighted. First, if most of the *pdf* of the parameter is out of the veering area, a draw of k_2 will mostly induce eigenvalues associated with a constant eigenvector as illustrated in Fig. 2(a). The eigenvectors obtained for the deterministic value of the input parameter can be used to estimate the corresponding random eigenvalues. The SMR first assumption is then validated. On the other hand, if the *pdf* of the parameter overlaps the veering area (see Fig. 2(b)), the eigenvector corresponding to an eigenvalue will depend on the drawn value of the parameter and it is necessary to take into account this variability to estimate the corresponding eigenvalues.

These two observations are reinforcing the SMR1 assumption whereby eigenvectors can be assumed deterministic depending on the eigenmode configuration. The *k*th eigenvalue is then approximated by Eq. (4). When the eigenvectors cannot be assumed deterministic, it is necessary to take into account their variability. A new refinement level is then proposed in the next section.

3. Refinement of the Stochastic Model Reduction

3.1. Improvement of SMR1: SMR2

When the eigenshapes variability increases, it is no longer possible to approximate the random eigenvectors as deterministic eigenvectors. In order to accurately estimate the corresponding eigenvalues, it is proposed to take into account the

eigenshapes variability with a Taylor expansion about the point $\boldsymbol{\gamma}(\theta) = \boldsymbol{\gamma}_0$. This improvement is referred to hereafter as SMR2.

The kth random eigenvalue $\lambda_k(\boldsymbol{\gamma}(\theta))$ and the kth eigenvector $\boldsymbol{\Phi}_k(\boldsymbol{\gamma}(\theta))$ given by its Taylor series expansion about the point $\mathrm{E}[\boldsymbol{\gamma}(\theta)] = \mathbf{1}$ can be written as:

$$\lambda_k(\theta) = \sum_{i=1}^{n} \gamma_i(\theta) \boldsymbol{\Phi}_k^{\top}(\boldsymbol{\gamma}(\theta)) \mathbf{K}_i \boldsymbol{\Phi}_k(\boldsymbol{\gamma}(\theta)) \tag{13}$$

$$\boldsymbol{\Phi}_k(\boldsymbol{\gamma}(\theta)) = \boldsymbol{\Phi}_k(\boldsymbol{\gamma}_0) + \sum_{i=1}^{n} \left.\frac{\partial \boldsymbol{\Phi}_k}{\partial \gamma_i}\right|_{\gamma_i=1} (\gamma_i(\theta) - 1) \tag{14}$$

The derivatives of each eigenvector remain to be determined. Many papers on the analysis and the calculation of eigen-derivatives of dynamic systems [24–26] are based on methods developed by Fox and Kapoor [20]. The next subsection defines the best suitable method to compute the eigenvector derivatives for the second refinement level of the SMR approach.

3.1.1. Methods to compute eigenvector derivatives

Of particular interest for design and shape optimization, model updating or even uncertainty analysis, the eigenvalue and eigenvector sensitivity computation has been extensively studied in the last decades. The aim of this section is to pick the most suitable existing method to compute the eigenvector derivatives for the SMR2 application. For this purpose, we have identified four types of approach to compute the eigenvector derivatives in the literature. This classification aims to be adapted to the SMR framework and its implicit requirements.

First, we identify modal superposition methods initiated by Fox and Kapoor works [20]. Fox and Kapoor present two main results about eigenvector derivatives. The first result is an expression of the eigenvector derivative depending only on the eigendata of the corresponding mode. This expression suffers from the required inverse of a $(n_d \times n_d)$ dense matrix, where n_d is the number of DoF of the system. To avoid the drawback of matrix inversion, Fox and Kapoor proposed a second expression based on the expansion of the eigenvector derivative on the eigenvector basis.

Several papers have followed the work initiated by Fox and Kapoor. Roger enlarges it to generalized non-symmetric eigenvalue problems [27]. Hirai and Kashiwaki focus on the case of structural modification with only a few controlled design variables [24]. The drawback of the Fox and Kapoor's expansion on the eigenvector basis is that it requires all the eigenvectors of the structure to be exact, and its accuracy decreases as the eigenvector basis is truncated. To circumvent these problems, numerous formulations have been proposed, including static corrections or iterative approaches as mentioned by Alvin [28]. Lin estimates the eigenvector derivatives by just using the modal parameters of that mode [29]. Nevertheless, Lin's method remains approximate and is inaccurate when the eigenvalues are too close. These methods are then not adapted to the SMR framework.

The second class of methods is based on a direct exact method termed Nelson's method. Nelson's [30] first proposed computing the eigenvector derivatives of nth-order symmetric or non-symmetric eigensystems by requiring only the left and right eigenvectors and the associated eigenvalue under consideration. The main advantage of this method is to require only the eigendata of the corresponding mode and to preserve the banded characteristics of the original eigensystem. Several works are based on the Nelson's method. Friswell [31,32] extends Nelson's method to eigenvalues and eigenvectors nth derivatives.

Ojalvo [33], Mills-Curran [34,35] and Dailey [36] have contributed to extend Nelson's method to the case of repeated eigenvalues. Nevertheless, their approaches involve second-order derivatives, which is inappropriate for SMR2 implementation. Chen [37] has raised that for some particular cases of repeated eigenvalues, Ojalvo, Mills-Curran and Dailey methods can be avoided, but these cases can not be generalized to SMR's scope. As mentioned by Lee [38], Nelson's method could be lengthy and complicated for finding eigenvector derivatives and clumsy for programming, but it is still faster than modal methods such as Fox and Kapoor's one. It could be implemented to compute the eigenvector derivatives of the SMR second refinement level.

Methods of the third class are iterative methods. Yoon and Belegundu [39] propose perturbing the input parameter vector of the system and solving the corresponding non-linear system with a Newton–Raphson technique. An iteration process is then used to converge toward the eigenvector derivatives. Alvin [28] uses the truncated Fox's method to initiate an iterative algorithm based on Preconditioned Conjugate Projected Gradient-based technique. Andrew [40] uses a simultaneous iteration technique for computing second-order partial derivatives. Nevertheless, due to the SMR framework, iterative methods are not favored.

The last class corresponds to semi-analytic methods. Jankovic [41] proposes calculating the exact nth eigenvalues and eigenvectors derivative of linear and non-linear eigenvalue problems for unrepeated eigenvalues. Olhoff and Lund [42,43] use "exact" numerical differentiation to compute design sensitivities of simple and multiple eigenvalues of complex structures. Mateus [44] considers the non-differentiability of multiple eigenvalues using thin-plate shell structures of arbitrary geometry. Although these methods provide an exact calculation (except for numerical round-off errors), they need to be implemented at the elementary level of the finite element solver. The SMR method aims to be non-intrusive, thus this kind of method is then excluded.

Particular attention could be paid to Lee's algebraic method to compute the eigenvector derivatives of a damped system [45,46]. This method does not really belong to one of the four identified classes, but appears to be a promising candidate to be implemented in SMR. This method is applied in an intrusive manner to compute derivatives of elementary matrices in the French opensource software *code_aster* [47], developed by the French company *Électricité de France*. The method is based on the eigenproblem equation and the orthonormal condition written in a matrix format. The orthonormal condition is quite different between a damped and an undamped system. The proposed expression of the eigenvector derivatives given in the dedicated papers [45,46] is adapted below to be implemented in the SMR second refinement level. The implemented method is detailed in the case of multiple eigenvalues and so it could be applied to the case of distinct eigenvalues. In particular, this method is well adapted for dealing with close eigenvalues.

3.1.2. Implemented method to compute eigenvector derivatives

In order to compute the eigenvector derivatives, a method proposed by Lee [45,46] is used. In this section, this method is briefly remembered in the specific case of undamped problem with multiple eigenvalues λ_m with m multiplicity (the case of single eigenvalue will follow from this results). Especially, this approach is based on the concept of adjacent eigenvectors, which allows us to deal with discontinuities of the eigenvectors since a parameter changed.

Let us consider the value p_0 of the parameter p corresponding to the nominal eigenvalue of multiplicity m. Associated with this eigenvalue, the eigenvectors $\mathbf{X}$ lead to an eigensubspace. Since a parameter p is varying from its nominal value to a value p', the eigenvectors $\mathbf{X}'$ lead to m distinct subspaces. In this context, since p tends to p_0, $\mathbf{X}'$ tends to $\mathbf{X}$, and the m distinct eigenvalues tend to the multiple eigenvalue λ_m. Such eigenvectors $\mathbf{X}$ are commonly designated as *adjacent* eigenvectors. Notice that these eigenvectors depend on which parameter is varying, *i.e.* specific adjacent eigenvectors must be taken into account for each considered parameter.

Firstly, the following eigenvalue problem, where $\mathbf{\Phi}_m$ is the $(n_d \times m)$ matrix of eigenvectors corresponding to λ_m and is defined as:

$$-\mathbf{M}\mathbf{\Phi}_m\mathbf{\Lambda}_m + \mathbf{K}\mathbf{\Phi}_m = 0 \tag{15}$$

where

$$\mathbf{\Lambda}_m = \lambda_m \cdot \mathbf{I}_m$$

The orthonormal condition is given by the following equation:

$$\mathbf{\Phi}_m^\top \mathbf{M}\mathbf{\Phi}_m = \mathbf{I}_m \tag{16}$$

Adjacent eigenvectors can be expressed in terms of $\mathbf{\Phi}_m$ by an orthogonal transformation such as:

$$\mathbf{X} = \mathbf{\Phi}_m\mathbf{T} \tag{17}$$

where $\mathbf{T}$ is an orthonormal transformation matrix of order m ($\mathbf{T}^\top\mathbf{T} = \mathbf{I}_m$). $\mathbf{X}$ also satisfies the orthonormal condition such as that in Eq. (16):

$$\mathbf{X}^\top\mathbf{M}\mathbf{X} = \mathbf{I}_m \tag{18}$$

Let us consider an other eigenvalue problem to find $\mathbf{X}$ and $\frac{\partial \mathbf{\Lambda}_m}{\partial p}$:

$$-\mathbf{M}\mathbf{X}\mathbf{\Lambda}_m + \mathbf{K}\mathbf{X} = \mathbf{0} \tag{19}$$

This problem is built by multiplying Eq. (15) by the matrix $\mathbf{T}$.

Differentiating the eigenvalue problem (15) with respect to the design parameter p, one has

$$-\frac{\partial \mathbf{M}}{\partial p}\mathbf{X}\mathbf{\Lambda}_m - \mathbf{M}\frac{\partial \mathbf{X}}{\partial p}\mathbf{\Lambda}_m - \mathbf{M}\mathbf{X}\frac{\partial \mathbf{\Lambda}_m}{\partial p} + \frac{\partial \mathbf{K}}{\partial p}\mathbf{X} + \mathbf{K}\frac{\partial \mathbf{X}}{\partial p} = \mathbf{0} \tag{20}$$

This equation leads to the next equation, as proposed by Lee:

$$(\mathbf{K} - \mathbf{\Lambda}_m\mathbf{M})\frac{\partial \mathbf{X}}{\partial p} = -\left(\frac{\partial \mathbf{K}}{\partial p} - \mathbf{\Lambda}_m\frac{\partial \mathbf{M}}{\partial p}\right)\mathbf{X} + \mathbf{M}\mathbf{X}\frac{\partial \mathbf{\Lambda}_m}{\partial p} \tag{21}$$

Premultiplying each side by $\mathbf{\Phi}_m^\top$ and substituting $\mathbf{X} = \mathbf{\Phi}_m\mathbf{T}$ into it gives a new eigenvalue problem such as:

$$\mathbf{D}\mathbf{T} = \mathbf{E}\mathbf{T}\frac{\partial \mathbf{\Lambda}_m}{\partial p} \tag{22}$$

where

$$\mathbf{D} = \mathbf{\Phi}_m^\top\left(-\lambda_m\frac{\partial \mathbf{M}}{\partial p} + \frac{\partial \mathbf{K}}{\partial p}\right)\mathbf{\Phi}_m \tag{23}$$

$$\mathbf{E} = -\mathbf{\Phi}_m^\top\mathbf{M}\mathbf{\Phi}_m = -\mathbf{I}_m \tag{24}$$

Henceforth, Lee's formulation [45,46] is used: it corresponds to an algebraic equation with symmetric coefficient matrix added side conditions.

Differentiating the orthonormal condition (Eq. (18)) of the adjacent eigenvectors gives:

$$\mathbf{X}^\top \mathbf{M} \frac{\partial \mathbf{X}}{\partial p} = -\frac{1}{2} \mathbf{X}^\top \frac{\partial \mathbf{M}}{\partial p} \mathbf{X} \tag{25}$$

One can then write the following single matrix equation combining Eqs. (21) and (25):

$$\begin{bmatrix} \mathbf{K} - \lambda_m \mathbf{M} & \mathbf{M}\mathbf{X} \\ \mathbf{X}^\top \mathbf{M} & \mathbf{0} \end{bmatrix} \begin{bmatrix} \frac{\partial \mathbf{X}}{\partial p} \\ \mathbf{0} \end{bmatrix} = \begin{bmatrix} -\left(\frac{\partial \mathbf{K}}{\partial p} - \boldsymbol{\Lambda}_m \frac{\partial \mathbf{M}}{\partial p} \right) \mathbf{X} + \mathbf{M}\mathbf{X} \frac{\partial \boldsymbol{\Lambda}_m}{\partial p} \\ -\frac{1}{2} \mathbf{X}^\top \frac{\partial \mathbf{M}}{\partial p} \mathbf{X} \end{bmatrix} \tag{26}$$

The coefficient matrix can be decomposed into upper and lower triangular forms, and then a forward and backward substitution scheme may be used to evaluate the components of $\frac{\partial \mathbf{X}}{\partial p}$.

Finally, Lee's algorithm could be summed up:

1) compute $\mathbf{D} = \boldsymbol{\Phi}_m^\top \left(-\lambda_m \frac{\partial \mathbf{M}}{\partial p} + \frac{\partial \mathbf{K}}{\partial p} \right) \boldsymbol{\Phi}_m$ and $\mathbf{E} = -\mathbf{I}_m$;
2) solve the eigenproblem $\mathbf{D}\mathbf{T} = \mathbf{E}\mathbf{T} \frac{\partial \boldsymbol{\Lambda}_m}{\partial p}$ and normalize so that $\mathbf{T}^\top \mathbf{T} = \mathbf{I}_m$;
3) let the columns of $\mathbf{X} = \boldsymbol{\Phi}_m \mathbf{T}$ be the new eigenvectors;
4) define $\mathbf{A} = \begin{bmatrix} \mathbf{K} - \lambda_m \mathbf{M} & \mathbf{M}\mathbf{X} \\ \mathbf{X}^\top \mathbf{M} & \mathbf{0} \end{bmatrix}$;
5) compute $F = \begin{Bmatrix} -\left(\frac{\partial \mathbf{K}}{\partial p} - \boldsymbol{\Lambda}_m \frac{\partial \mathbf{M}}{\partial p} \right) \mathbf{X} + \mathbf{M}\mathbf{X} \frac{\partial \boldsymbol{\Lambda}_m}{\partial p} \\ -\frac{1}{2} \mathbf{X}^\top \frac{\partial \mathbf{M}}{\partial p} \mathbf{X} \end{Bmatrix}$;
6) compute $\begin{bmatrix} \frac{\partial \mathbf{X}}{\partial p} \\ \mathbf{0} \end{bmatrix} = [\mathbf{A}]^{-1} F$.

The proof of the numerical stability (*i.e.* the non-singularity of the matrix $\mathbf{A}$) of this algorithm is detailed analytically in [45] in the case of distinct eigenvalues and in [46] in the case of multiple eigenvalues.

3.1.3. Comparison with the second-order perturbation method

The first refinement level of the SMR approach could be seen as a first-order perturbation method as shown in section 2.2.3. The second-order perturbation method is also widespread in the literature [8]. This section enables us to compare the second-order perturbation method and the second refinement level of the SMR approach.

Let us consider the random eigenvalue problem as defined in Eq. (1). The mass matrix $\boldsymbol{M}(\boldsymbol{\gamma}) : \mathbb{R}^n \mapsto \mathbb{R}^{n_d \times n_d}$ and the stiffness matrix $\boldsymbol{K}(\boldsymbol{\gamma}) : \mathbb{R}^n \mapsto \mathbb{R}^{n_d \times n_d}$ are assumed to be smooth, continuous and at least twice differentiable functions of a random vector $\boldsymbol{\gamma} \in \mathbb{R}^n$ representing the n input parameters of the vibrational system. According to the second–order perturbation method, the kth random eigenvalue $\lambda_k(\boldsymbol{\gamma})$ could be approximated through its second-order Taylor expansion about the mean point $\boldsymbol{\gamma} = \boldsymbol{\gamma}_0$. This approximation is referred as $\lambda^{\text{pert.2}}$:

$$\lambda_k(\boldsymbol{\gamma}) \approx \lambda_k^{\text{pert.2}} = \lambda(\boldsymbol{\gamma}_0) + \sum_{i=1}^{n} \left(\left. \frac{\partial \lambda_k}{\partial \gamma_i} \right|_{\boldsymbol{\gamma} = \boldsymbol{\gamma}_0} (\gamma_i - \gamma_{i0}) \right) + \sum_{i=1}^{n} \sum_{j=1}^{n} \left(\frac{1}{2} \left. \frac{\partial^2 \lambda_k}{\partial \gamma_i \partial \gamma_j} \right|_{\boldsymbol{\gamma} = \boldsymbol{\gamma}_0} (\gamma_i - \gamma_{i0})(\gamma_j - \gamma_{j0}) \right) \tag{27}$$

The eigenvalue's first derivative is presented in Eq. (11). This derivative involves only the sensitivity of the mass and stiffness matrices at the mean value of the input random vector $\boldsymbol{\gamma}$. Providing the eigenvalues are distinct, Plaut and Huseyin [48] have shown that the expression of the second derivative is:

$$\begin{aligned} &\frac{\partial^2 \lambda_k}{\partial \gamma_i \partial \gamma_j}(\boldsymbol{\gamma}) \\ &= \boldsymbol{\Phi}_k(\boldsymbol{\gamma})^\top \left[\frac{\partial^2 \boldsymbol{K}(\boldsymbol{\gamma})}{\partial \gamma_i \partial \gamma_j} - \lambda_k(\boldsymbol{\gamma}) \frac{\partial^2 \boldsymbol{M}(\boldsymbol{\gamma})}{\partial \gamma_i \partial \gamma_j} \right] \boldsymbol{\Phi}_k(\boldsymbol{\gamma}) - \left(\boldsymbol{\Phi}_k(\boldsymbol{\gamma})^\top \frac{\partial \boldsymbol{M}(\boldsymbol{\gamma})}{\partial \gamma_i} \boldsymbol{\Phi}_k(\boldsymbol{\gamma}) \right) \left(\boldsymbol{\Phi}_k(\boldsymbol{\gamma})^\top \mathcal{G}_{kj}(\boldsymbol{\gamma}) \boldsymbol{\Phi}_k(\boldsymbol{\gamma}) \right) \\ &\quad - \left(\boldsymbol{\Phi}_k(\boldsymbol{\gamma})^\top \frac{\partial \boldsymbol{M}(\boldsymbol{\gamma})}{\partial \gamma_j} \boldsymbol{\Phi}_k(\boldsymbol{\gamma}) \right) \left(\boldsymbol{\Phi}_k(\boldsymbol{\gamma})^\top \mathcal{G}_{ki}(\boldsymbol{\gamma}) \boldsymbol{\Phi}_k(\boldsymbol{\gamma}) \right) + 2 \sum_{\substack{r=1 \\ r \neq k}}^{N} \frac{\left(\boldsymbol{\Phi}_r(\boldsymbol{\gamma})^\top \mathcal{G}_{ki}(\boldsymbol{\gamma}) \boldsymbol{\Phi}_k(\boldsymbol{\gamma}) \right) \left(\boldsymbol{\Phi}_r(\boldsymbol{\gamma})^\top \mathcal{G}_{kj}(\boldsymbol{\gamma}) \boldsymbol{\Phi}_k(\boldsymbol{\gamma}) \right)}{\lambda_k(\boldsymbol{\gamma}) - \lambda_r(\boldsymbol{\gamma})} \end{aligned} \tag{28}$$

where

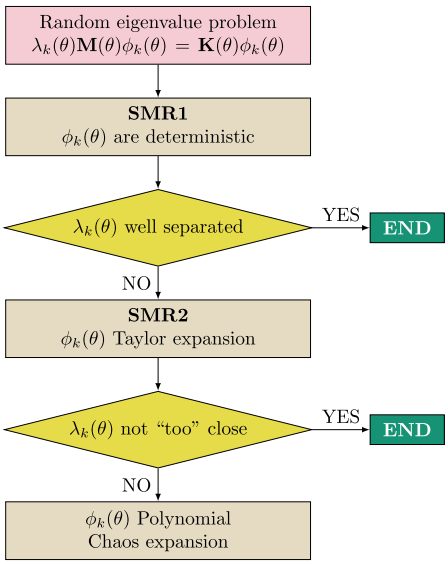

Fig. 3. SMR approach for eigenvalue problem resolution.

$$\mathcal{G}_{ki}(\boldsymbol{\gamma}) = \left[\frac{\partial \boldsymbol{K}(\boldsymbol{\gamma})}{\partial \gamma_i} - \lambda_k(\boldsymbol{\gamma})\frac{\partial \boldsymbol{M}(\boldsymbol{\gamma})}{\partial \gamma_i}\right] \tag{29}$$

This expansion could be rewritten as a second-order polynomial of the input random parameters:

$$\lambda_k^{\text{pert.2}} = a_k + \sum_{i=1}^{n} b_{ki}\gamma_i + \sum_{(i,j)\in[\![1;n]\!]^2} c_{kij}\gamma_i\gamma_j \tag{30}$$

With the second refinement level of the SMR approach, the kth random eigenvalue is approximated by taking into account the variability of the kth eigenvector with a first-order Taylor expansion.

$$\lambda_k^{\text{SMR2}} = \sum_{i=1}^{n} \gamma_i \boldsymbol{\Phi}_k^{\top}(\boldsymbol{\gamma})\mathbf{K}_i\boldsymbol{\Phi}_k(\boldsymbol{\gamma}) \tag{31}$$

$$= \sum_{i=1}^{n} \gamma_i \left(\boldsymbol{\Phi}_k(\boldsymbol{\gamma}_0) + \sum_{j=1}^{n} \left.\frac{\partial \boldsymbol{\Phi}_k}{\partial \gamma_j}\right|_{\gamma_j=1} (\gamma_j - 1)\right)^{\top} \mathbf{K}_i \left(\boldsymbol{\Phi}_k(\boldsymbol{\gamma}_0) + \sum_{j=1}^{n} \left.\frac{\partial \boldsymbol{\Phi}_k}{\partial \gamma_j}\right|_{\gamma_j=1} (\gamma_j - 1)\right) \tag{32}$$

On this basis, the approximated eigenvalue λ_k^{SMR2} could be written as a polynomial of the input random parameters:

$$\lambda_k^{\text{SMR2}} = e_k + \sum_{i=1}^{n} f_{kij}\gamma_i + \sum_{(i,j)\in[\![1;n]\!]^2} g_{kij}\gamma_i\gamma_j + \sum_{(i,j,l)\in[\![1;n]\!]^3} h_{kijl}\gamma_i\gamma_j\gamma_l \tag{33}$$

As shown in section 3.1.2, the eigenvector derivatives require only the eigendata of the corresponding mode, the mass and stiffness matrices and their sensitivities. On the other hand, the second-order perturbation method involves the first and second derivatives of the mass and stiffness matrices, and all the eigenvectors of the system need to be computed. The computation of λ_k^{SMR2} is then cheaper than $\lambda_k^{\text{pert.2}}$. Moreover, in comparison with the $\lambda_k^{\text{pert.2}}$ approximation, the eigenvalue λ_k^{SMR2} is described with a polynomial of higher degree. The SMR2 approximation will better fit the response surface corresponding to the exact random eigenvalue.

3.2. The SMR resolution approach

For real structures, the set of random eigenvalues will contain either eigenvalues corresponding to almost deterministic eigenvectors and eigenvalues corresponding to random eigenvectors. The two refinement levels of the SMR method have to be jointly used to ensure the best estimation of the whole set of random eigenvalues. To this purpose, a simple resolution approach is summarized in Fig. 3. This approach consists in adapting the invested computational resources to each random eigenvalue. First, all random eigenvalues are approximated with SMR1, assuming that all eigenvectors are deterministic. This first step provides an initial estimation of all eigenvalues. The issue is then to identify when the SMR1 assumption is

validated or it is necessary to refine the approximation. The idea, which appears in different papers about the perturbation methods [8], eigendata sensitivity [29] or eigenloci curve veering [22,23], is to distinguish well-separated eigenvalues from close ones. In the case of well-separated eigenvalues, the eigenshape sensitivity with respect to the input parameters is small [22], the SMR1 assumption is then validated and the corresponding random eigenvalues will be accurately estimated with SMR1. In the case of random eigenvalues not clearly identified as well separated, SMR2 is used to estimate a better approximation of the eigenvalues. Thus, the SMR2 method is applied on a reduced set of eigenvalues. Notice that, the first-order Taylor expansion of one eigenvector using Lee's algorithm [45,46] presented in section 3.1.2 is used to compute the eigenvector derivatives.

As with SMR1, the quality of the SMR2 estimation decreases when random eigenvalues are getting closer. So the use of first-order Taylor expansions could be insufficient to estimate random eigenvectors because their randomness is not adequately taken into account. A second-order Taylor expansion seems to be inappropriate due to the second-order derivation of the random eigenvectors. In order to overcome this drawback, the random eigenvectors could be modeled by their polynomial chaos (PC) expansions. The coefficients of the eigenvector PC expansion are rather complex to determine [14]. Therefore, the PC expansion is used only for the last random eigenvalues for which the SMR2 accuracy is questionable.

3.3. Definition of a proximity factor

The efficiency of the proposed approach now depends on the ability to qualify the proximity of two random eigenvalues. The notion of "close eigenvalue" appears in different papers about eigenvalue curve veering [22,23], statistical energy analysis [49], eigenvalues and eigenvectors derivatives [29] and, a fortiori, random eigenvalue problems [8]. In a most general statistics framework, the use of a specific distance measure could be used such as the Mahalanobis distance [50,51]. Even if both close and well-separated cases are dealt with systematically, the limit between these two configurations is not always handled for random eigenvalue problems. Du Bois et al. [23] propose a modal coupling factor analogous to the coupling factor of Perkins and Mote [21]. This factor is based on the stiffness and mass matrix sensitivities, which are deterministic and available from commercial software, but it relates the coupling between two eigenvalues only when a single parameter is varying. An indicator could be constructed on this basis in order to take into account the whole set of input random parameters, but it would be the object of future work. Although the correlation between eigenvalues could be considered [52], the implicit assumptions of SMR1 lead to uncorrelated eigenvalues. Therefore the proximity indicator between two random eigenvalues should be built without correlation terms (see Eq. (34)). In this paper, an indicator inspired by the statistical overlap factor of Manohar and Keane [49] seems to be more suitable because of a low computational cost. The statistical overlap is defined as the ratio between the standard deviation of the ith natural frequency and the mean modal spacing. In order to take into account a potential difference between the standard deviation of two random eigenvalues, the proximity factor (PF) of two random eigenvalues λ_i, λ_{i+1} is defined as:

$$PF(\lambda_i) = \frac{2(\sigma[\lambda_i] + \sigma[\lambda_{i+1}])}{\mathrm{E}[\lambda_{i+1}] - \mathrm{E}[\lambda_i]} \tag{34}$$

As the expectation and the standard deviation of every random eigenvalue are estimated through the SMR methods, the proximity factor is obtained directly. The proximity factor allows us to qualify the quality of the estimation computed with the SMR methods. When the proximity factor is greater than a limit value, initially assumed as $PF > 1$, the corresponding eigenvalues are assumed to be closely spaced and the SMR assumptions (random eigenvectors are deterministic for SMR1 and have small variations for SMR2) are not valid. As a result, the confidence in the SMR results must be studied depending on the value of the proximity factor.

3.4. Stochastic modeling of the parameters

The SMR methods have been established, it now remains to construct, as objectively as possible, the probability law of the input parameters, for example their probability density function (*pdf*). Denoting a random parameter by $X(\theta)$, some available information has to be taken into account [53], for instance,

- $X(\theta)$ has to be a positive-valued random variable (Young's modulus),
- $X(\theta)$ has to be a second-order random variable, i.e. $\mathrm{E}[X^2(\theta)] < \infty$,
- the mean value of $X(\theta)$ is given and denoted by $\mathrm{E}[X(\theta)] = \overline{x} > 0$,
- the solution to the problem, here $\lambda(\theta)$, has to be a second-order random variable

When other information is available, for example experimental data, the *pdf* of the parameter could be constructed through the maximum likelihood principle. Otherwise, if no other information is available, the *pdf* could be constructed through the maximum entropy principle [54]. For example, according to the maximum entropy principle, a real-valued random variable X such as $\mathrm{Supp}(X) =]0, +\infty[$, $\mathrm{E}[X] = m_x$ and $\mathrm{Var}[X] = \sigma_x^2$ follows a Gamma distribution.

For a given material, Young's modulus is randomly varying, its expectation and standard deviation are known and its support is positive. Young's moduli can be modeled as random variables with Gamma distribution. If $Y_i \rightsquigarrow \mathrm{Gamma}(\alpha_i, \beta_i) = \Gamma(\alpha_i, \beta_i)$, then $\mathrm{E}[Y_i] = \alpha_i\beta_i$ and $\mathrm{Var}[Y_i] = \alpha_i\beta_i^2$. Therefore, α_i and β_i are given by:

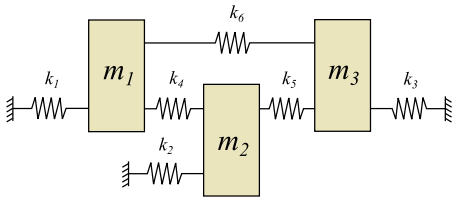

Fig. 4. Three-degrees-of-freedom undamped spring-mass random system.

$$\alpha_i = \left(\frac{\mathrm{E}[Y_i]}{\sigma_{Y_i}}\right)^2 \quad \text{and} \quad \beta_i = \frac{\sigma_{Y_i}^2}{\mathrm{E}[Y_i]} \tag{35}$$

The scaling property of the Gamma distribution, whereby if $Y_i \rightsquigarrow \mathrm{Gamma}(\alpha_i, \beta_i) = \Gamma(\alpha_i, \beta_i)$, then for any $c > 0$, $cY_i \rightsquigarrow \mathrm{Gamma}(\alpha_i, c\beta_i)$, allows us to write the input random variables of the problem γ_i as a function of the coefficient of variation $\delta_i = \frac{\sigma_{Y_i}}{\mathrm{E}[Y_i]}$ of Young's moduli:

$$\gamma_i \rightsquigarrow \mathrm{Gamma}\left(\frac{1}{\delta_i^2}, \delta_i^2\right) \tag{36}$$

The summation property gives the distribution of the sum of independent random variables $(Y_i)_{1\leq i\leq n}$ with $\mathrm{Gamma}(\alpha_i, \beta)$ distributions for $i = 1, ..., n$ and same scale parameter β:

$$\sum_{i=1}^{n} Y_i \rightsquigarrow \mathrm{Gamma}\left(\sum_{i=1}^{n} \alpha_i, \beta\right) \tag{37}$$

4. First application: a three-DoF system

4.1. System modeling

In order to illustrate the SMR method, a simple three-degrees-of-freedom (DoF) undamped spring-mass system is considered. This example is taken from [32] and [8], and presented in Fig. 4. The advantage of this example is to easily drive the system eigenvalues with only one of the input random parameters. This allows us to characterize the quality of the SMR method when eigenvalues are well separated or close.

The mass and stiffness matrices of this three-DoF system are given by:

$$\mathbf{M} = \begin{bmatrix} m_1 & 0 & 0 \\ 0 & m_2 & 0 \\ 0 & 0 & m_3 \end{bmatrix} \quad \text{and} \quad \mathbf{K} = \begin{bmatrix} k_1 + k_4 + k_6 & -k_4 & -k_6 \\ -k_4 & k_2 + k_4 + k_5 & -k_5 \\ -k_6 & -k_5 & k_3 + k_5 + k_6 \end{bmatrix} \tag{38}$$

It is assumed that only spring stiffnesses k_i with $i = \{1, \ldots, 6\}$ are randomly varying and the vector of the random stiffnesses is noted $\mathbf{x} = [k_1, \ldots, k_6]^\top$. Each random stiffness is assumed to have a Gamma distribution with expectation $\overline{k_i} = 1$ N·m^{-1} for $i = \{1, \ldots, 5\}$. The mean value of the k_6 random stiffness is fixed at $\overline{k_6} = 3$ N·m^{-1} for simulations with well-separated eigenvalues, and $\overline{k_6} = 1.275$ N·m^{-1} in the case of close eigenvalues. The standard deviation of each random stiffness is $\sigma_{k_i} = 0.15$ N·m^{-1} for $i = \{1, \ldots, 6\}$.

A Monte Carlo simulation allows us to compute the *pdf* and the two first statistical moments of the random eigenvalues. The samples of the six independent Gamma random variables k_i for $i = \{1, \ldots, 6\}$ are generated and the eigenvalues are computed from the eigenvalue problem (1). A simulation with 30000 samples guaranties the estimation of the two first statistical moments with an error range of $\pm 0.1\%$. The results from this Monte Carlo simulation are considered as reference to evaluate the quality of the SMR method.

4.2. All eigenvalues are well separated

First, the case of well separated eigenvalues is considered. This assumption corresponds to $\overline{k_i} = 1$ N·m^{-1} for $i = \{1, \ldots, 5\}$ and $\overline{k_6} = 3$ N·m^{-1}. In this case, the random eigenshapes are assumed to be deterministic and the two first moments of the random eigenvalues are directly obtained through expressions (6) and (9). The relative error of the ith statistical moment estimated with SMR1 and denoted $\widehat{m}_i^{\mathrm{SMR1}}$ is given by:

$$\mathit{Error}\left(\widehat{m}_i^{\mathrm{SMR1}}[\lambda_k]\right) = \epsilon\left(\widehat{m}_i^{\mathrm{SMR1}}[\lambda_k]\right) = \left|\frac{\widehat{m}_i^{\mathrm{SMR1}}[\lambda_k] - \widehat{m}_i^{MC}[\lambda_k]}{\widehat{m}_i^{MC}[\lambda_k]}\right| \tag{39}$$

Table 1
Relative error in the estimation of the two first moments with SMR1.

	λ_1	λ_2	λ_3
Expectation relative error	$3.6 \cdot 10^{-3}$	$1.9 \cdot 10^{-3}$	$1.4 \cdot 10^{-3}$
Standard deviation relative error	$6.1 \cdot 10^{-3}$	$6.6 \cdot 10^{-3}$	$2.2 \cdot 10^{-3}$

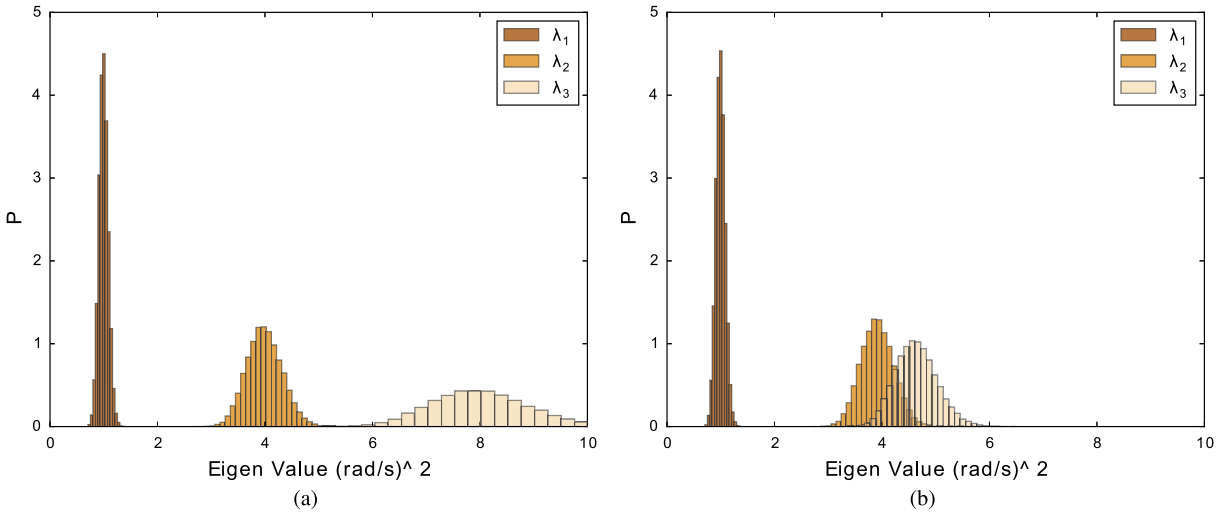

Fig. 5. Superposition of all eigenvalue marginal density functions. (a) All eigenvalues are well separated. (b) Two eigenvalues are close.

The relative error in the estimations of the first two statistical moments with SMR1 for the 3-DoF system are provided in Table 1. It can be noticed that the error is less than 0.4% for the expectation estimation of each random eigenvalue and less than 0.7% for the standard deviation. The reference moments from the Monte Carlo simulation need 30000 resolutions of the eigenvalue problem corresponding to each realization of the set of input random stiffness values. The SMR1 method requires only one deterministic resolution of the eigenvalue problem for the same accuracy. Note that SMR1 is sufficient to estimate the two first statistical moments of all eigenvalues, because all eigenvalues are well separated.

4.3. Two close eigenvalues

By fixing the expectation of the sixth random stiffness to $\overline{k_6} = 1.275$ N·m^{-1}, the first random eigenvalue of the three-DoF system remains significantly identical to the previous case but the second and third random eigenvalues are now closely spaced. Thus the SMR1 method could be applied to close random eigenvalues and the benefits of the enhanced method SMR2 could be illustrated. The marginal density functions of the three random eigenvalues of the system are plotted on a same graph (Fig. 5b). It should be noted that this representation is used to illustrate the proximity of two random eigenvalues.

The relative error in the estimation of the two first statistical moments with SMR1 and SMR2 is presented in Fig. 6. This figure illustrates the degradation of the SMR1 results when the eigenvalues are close. The relative error on the estimation of the statistical moment of the second and third random eigenvalues with SMR1 is nearly 10 times greater than in the case of well-separated eigenvalues. The enhancement of the SMR2 method allows us to decrease the relative errors respectively to $5.9 \cdot 10^{-3}$ and $5.1 \cdot 10^{-3}$ for the estimation of the second and third eigenvalue expectations. For the standard deviation estimation of the second and third eigenvalues, the relative errors with SMR2 are, respectively, $5.7 \cdot 10^{-3}$ and $7.1 \cdot 10^{-3}$.

For this test case, the first statistical moments of the random eigenvalues are also estimated with the second-order perturbation method. The estimation of the expectation with the second-order perturbation method is better than the estimation with SMR2. Nevertheless, as the expectation is estimated with an error less than 1% with the two methods, we can be satisfied with the SMR2 estimation. Concerning the estimation of the standard deviation, the second-order perturbation method is by far the less accurate one. While the standard deviation is estimated with an error less than 1% with SMR2, the error with the second-order perturbation method is up to 5%. This is due to the shape of the exact eigenvalue response surface, which is better fitted by the SMR2 approximation than the second-order perturbation, as illustrated in Fig. 7. This figure presents the exact response surface of the second and third eigenvalues when the first five stiffness parameters $k_1, \ldots, k_5$ are fixed at their mean value $k_i = 1$ N·m^{-1} and k_6 varies between 0 and 2 N·m^{-1}. The exact response surface, named *Ref* for reference, is compared to the approximated response surface obtained with SMR1, SMR2, and the second-order perturbation method. This agrees with the conclusion of section 3.1.3. In order to approximate the random eigenvalue, the second-order perturbation method is equivalent to a second-order polynomial function of the input random

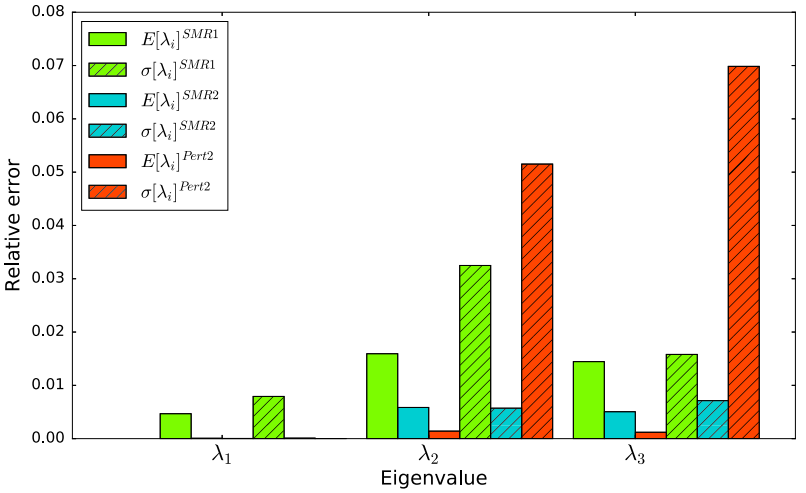

Fig. 6. Relative error on the estimation of the two first statistical moments.

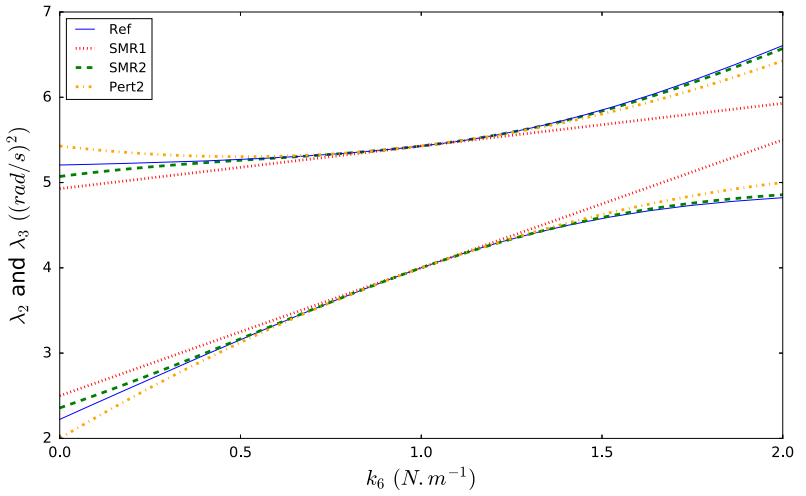

Fig. 7. Response surface of the second and third eigenvalues computed with the exact resolution (*Ref*), SMR1, SMR2 and second-order perturbation method.

parameters. On the other hand, with SMR2, the random eigenvalues are approximated with higher -order polynomial functions and, due to the shape of the exact eigenvalue loci, the SMR2 approximation is a better fit. Fig. 7 is equivalent to a slice of the eigenvalue response hyper-surfaces obtained with the exact resolution and the three approximated methods. The eigenvalues response hypersurfaces are dependent on six parameters. Representing it on a plane figure is quite unwieldy, that is why the development is limited to the case of a single varying parameter. Nevertheless, the conclusion still stand for more than one variable.

4.4. Proximity factor characterization

4.4.1. Indicator of the SMR methods quality

In order to illustrate the quality of the method (with only one deterministic calculation) for the case of close or well-separated random eigenvalues, the proposed methods have been applied to the three-DoF system for different eigenvalue configurations. The input random parameters keep the same characteristics (expectation and standard deviation) as defined in section 4.1, except for the k_6 expectation, which is varying between $1,275$ N·m^{-1} and 3 N·m^{-1}. This allows us to bring the second and third random eigenvalues closer. Fig. 8 represents the relative error in the estimation of the expectation and the standard deviation of the 2nd and 3rd random eigenvalues of the three-DoF system. It illustrates the decrease in the quality of the SMR1 and SMR2 methods when the proximity factor is increasing.

It can be noticed that, when the proximity factor is increasing, the quality of the first moments' estimation decreases. For proximity factors less than 1, the relative error of the SMR1 method is less than 0.7% for the expectation estimation and less than 3% for the standard deviation. The same quality is obtained for higher proximity factors with the SMR2 method; then, for a given quality, the limit value of the proximity factor should be adapted to the employed method.

We can then conclude that the proximity factor is a good quality indicator for the SMR1 and SMR2 methods.

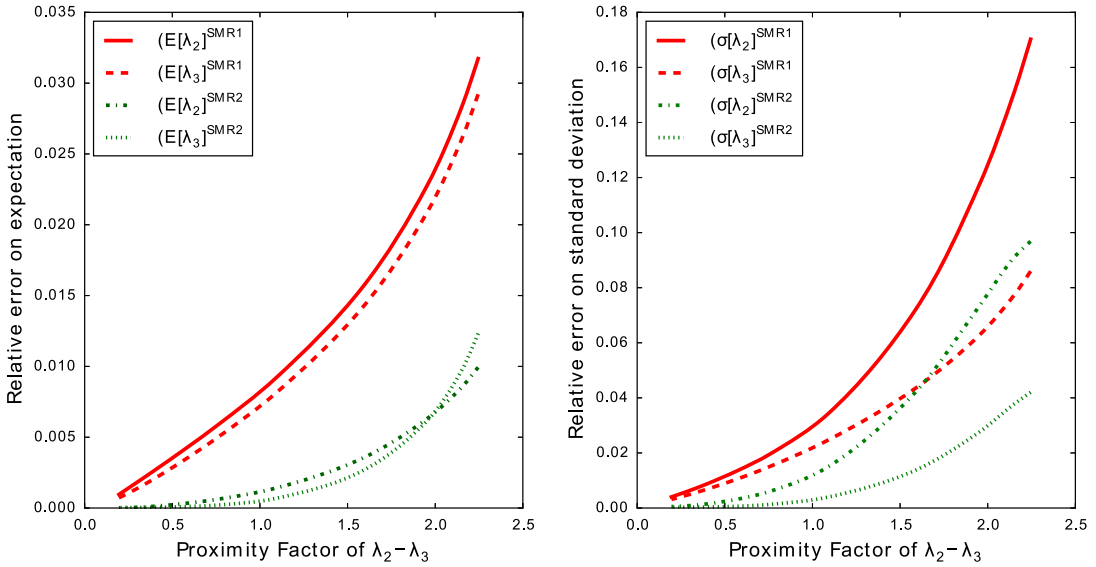

Fig. 8. Error on the estimation of the first moments when PF increases.

4.4.2. Error on the estimation of the proximity factor

The proximity factor qualifies the quality of the SMR methods; nevertheless, the error of the first moments' estimation leads to a certain approximation of the proximity factor itself. Two eigenvalues are considered close depending on their expectation and on their standard deviation. It is now proposed to study the estimation of the proximity factor with SMR1 and SMR2 when the expectation and the standard deviation of the corresponding random eigenvalues are varying.

Fig. 9 shows the proximity factor of the second and third random eigenvalues estimated with the SMR1 and SMR2 methods when the two random eigenvalues are getting closer. In order to characterize the proximity factor, a set of 120 configurations has been simulated. For each simulation, the random input stiffness $k_6(\theta)$ is defined as a Gamma random variable with expectation $\mathrm{E}[k_6]$, which assumes 10 values between 1.275 and 4, and the coefficient of variation $\delta[k_6] = \sigma[k_6]/\mathrm{E}[k_6]$ assumes 12 values between 0.05 and 0.3. The reference values of PF are obtained through Monte Carlo simulations with 30000 samples, and are extrapolated to obtain the blue surface (PF_2^{exact}) in Fig. 9. It can be observed that for $PF < 1$, corresponding to the red plane of the equation $z = 1$, the estimations of PF with SMR1 and SMR2 are close to reference values. In order to quantify the error in the estimation of PF, Fig. 10 presents the relative error between the reference proximity factor and its estimations obtained with SMR1 and SMR2. The limit criterion $PF = 1$ is represented by the line with the equation $y = x$. To illustrate the trend of the relative error of PF, a cubic interpolation is used to map the field of study, which explains the lack of information in the upper left area.

As might have been expected, over the limit value $PF = 1$, the estimation of PF is less accurate. Nevertheless, the purpose is to identify the validity domain of the SMR1 and SMR2 methods, i.e. to identify with a certain precision the limit value of PF above which the method used to compute the random eigenvectors has to be refined. It can be noticed that the error in the estimation of the limit value $PF = 1$ with SMR1 is less than 10%, while the error is around 1% with SMR2. It could therefore be considered that PF estimated with SMR1 allows us to identify when SMR2 needs to be used. The PF estimated with SMR2 is more reliable and could allow us to identify a higher limit value of PF above which the SMR2 method needs to be refined, for example by considering the eigenvector polynomial chaos expansion [14].

4.4.3. Discussion

It should be kept in mind that, by definition, the PF estimation is more sensitive to the random eigenvalue proximity than the estimation of the two first moments themselves. Nevertheless, it is not critical, because the main purpose is to choose the best suitable method to estimate the first moments. Considering the SMR1 results, the PF limit value $PF = 1$ is estimated with an error close to 8%, but the corresponding expectation and standard deviation are estimated with relative errors respectively less than 0.8% and 3%. Even if the PF is not estimated with a good precision, the error in the first moments estimated with SMR1 is acceptable. The same argument can be made for the PF estimation with SMR2.

To ensure a better estimation of PF, the limit value criterion could be decreased. In Fig. 10, this is equivalent to a decrease in the slope of the given red line. Nevertheless, the number of random eigenvalues considered to be close would increase, and it would be the same for the global computational cost, increased by refining the method more often.

The PF limit value criterion is then a key point of the SMR method. Decreasing the limit value of PF allows us to increase the quality of the solution by refining the method used to compute the random eigenvector for a larger number of random eigenvalues, but it implies a bigger investment in computational cost. As a partial conclusion, even if it is based on statistical

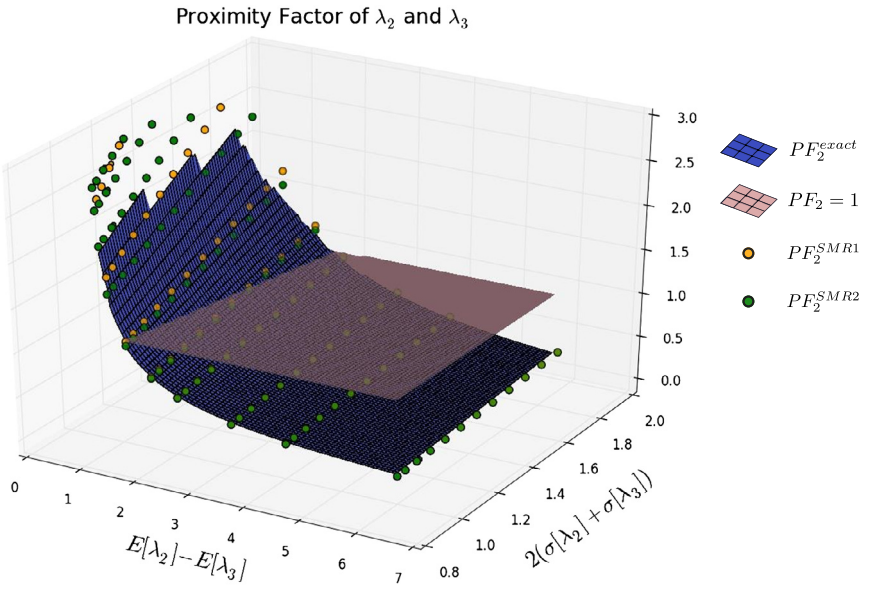

Fig. 9. Estimation of the proximity factor when λ_2 and λ_3 are getting closer.

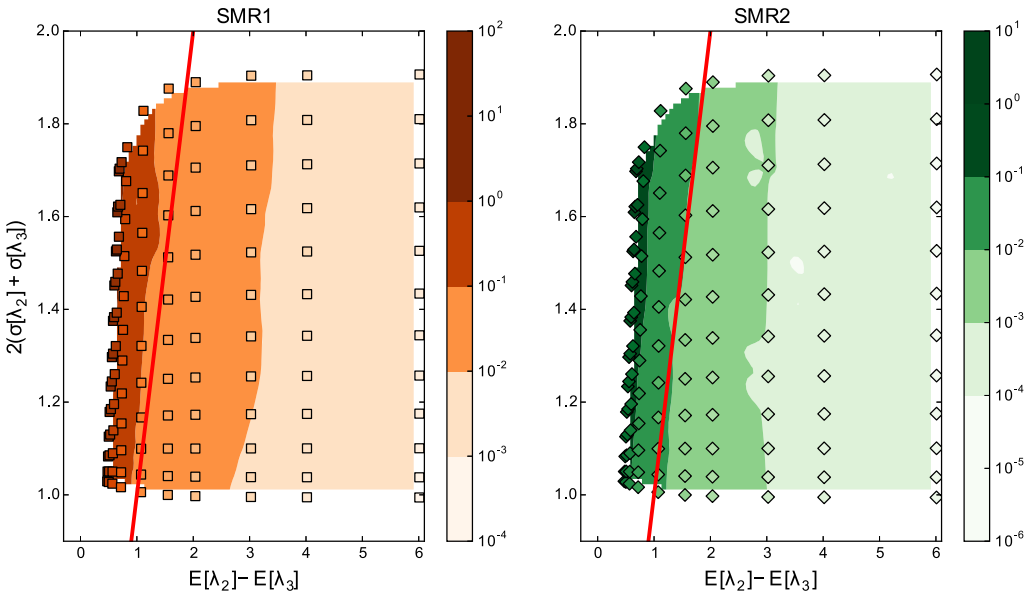

Fig. 10. Relative error of the proximity factor respectively computed with SMR1 and SMR2.

moments' estimations, the proximity factor is able to identify a validity domain of the two SMR methods. Its capability is based on the choice of the limit value, which depends on the required quality or the available computation resources.

5. Application to a frame

In this section, an application of the SMR approach is proposed on a structure consisting of several sub-structures with Young modulus and mass randomly varying. This example could be extended to a bolted assembly including piezoelectric devices. Before applying the SMR approach to an industrial test case (See section 6), this example will be an opportunity to apply it on a simple structure solved using finite element analysis and containing only a few degrees of freedom.

5.1. System modeling

The studied structure, presented in Fig. 11, is a frame comprised of three substructures with two random Young's moduli, denoted by $Y_1(\theta)$ and $Y_2(\theta)$, and one deterministic, denoted by Y_3. The three substructures are beams with the same

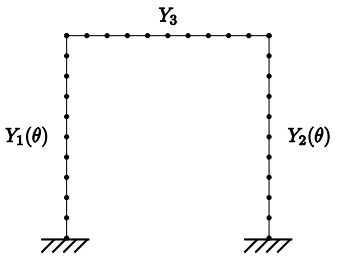

Fig. 11. Definition of the three beams frame.

geometrical properties: length 250 mm, width 10 mm, and thickness 1 mm. The three beams are assumed to have the same density $\rho = 2800$ kg·m^{-3}. The Young's moduli expected values are $\overline{Y_1} = 75$ GPa, $\overline{Y_2} = 75$ GPa and $\overline{Y_3} = 20$ GPa. The frame is modeled by finite elements with 30 beams elements and 3 DoF at each node. The base of the frame is assumed to be clamped, the DoF of the corresponding nodes are then set, and the complete system has 87 DoF.

The two input random parameters of the structure, $Y_1(\theta)$ and $Y_2(\theta)$, are modeled as independent random variables with Gamma distribution. Their expectation and standard deviation are respectively $\mathrm{E}[Y_1] = \mathrm{E}[Y_2] = 75$ GPa and $\sigma[Y_1] = \sigma[Y_2] = 5$ GPa (corresponding to a coefficient of variation $\delta = \sigma[Y_i]/\mathrm{E}[Y_i] = 1/15$) and correspond to small variations of the Young moduli.

A Monte Carlo simulation with 30000 samples allows us to compute the *pdf* of each random variable of interest. It constitutes the reference framework to compare the results from the SMR method.

5.2. Numerical results

5.2.1. Preliminary observations: illustration of the SMR founding assumption

The Monte Carlo simulation allows us to estimate the first five random eigenfrequencies through 30000 draws of the two input Young's moduli. Fig. 12 shows the marginal density functions of the first five random eigenvalues and corresponding eigenvectors of the frame. It can be noticed that the first, second, and fifth eigenshapes do not vary significantly, while the third and fourth eigenshapes have high variations. This illustrates the SMR1 assumption that, under certain conditions, the random eigenvectors of the structure could be considered as deterministic. The behavior of the 3rd and 4th random eigenmodes should be related to the relative "location" of the random eigenvalues. An overlap could be observed, representing their marginal *pdf* on the same axis.

5.2.2. First five random eigenvalues of the frame

Fig. 13 shows the marginal *pdf* obtained with SMR1 and SMR2 in comparison with the marginal *pdf* from the Monte Carlo simulation. For the three well separated eigenfrequencies, the SMR1 and SMR2 methods properly fit the reference marginal *pdf*. In the case of two close eigenfrequencies, as illustrated by the 3rd and 4th eigenfrequencies, the SMR1 method does not accurately estimate the marginal *pdf* whereas the SMR2 method is still fitting the reference results.

The relative errors of the first two statistical moments are presented in Figs. 14 and 15. It can be noticed that, for the three random eigenfrequencies that are well separated, the relative error in the estimation of the two first moments with the SMR1 method is less than 0.5%. The SMR2 method obviously gives better results, but it is not necessary to invest in more complex computations, while SMR1 results are sufficient. The table below the error diagrams 14 and 15 presents the approximation of the proximity factor computed from the first moments estimations of the SMR1 and SMR2 methods compared to the reference proximity factor from Monte Carlo simulation. The proximity factor between the first and second random eigenfrequencies corresponds to the cell between these two eigenfrequencies and so on. The cell color is purple if the proximity factor is under the limit value $PF = 1$, and is orange when it is over this limit. It can be noticed that PF_{SMR1} correctly identifies the two close random eigenfrequencies for which the method has to be refined.

5.2.3. First twenty-five random eigenvalues of the frame

The frame application allows us to test the SMR methods on higher eigenfrequencies. The estimations of the first two statistical moments of the 25 first random eigenfrequencies are presented in Figs. 16 and 17. It can be noticed that the relative error of the expectation is less than 1.5% for SMR1 and 1.1% for SMR2, and the relative error of the standard deviation is less than 20% for SMR1 and 14% for SMR2. Globally, the relative error increases with the frequency. Some random eigenvalues deserve detailed examination.

- The 6th and 19th random eigenfrequencies present an error in the estimation of their first two statistical moments with SMR1, whereas SMR2 gives much better results. The error in the expectation ω_6 estimated with SMR1 is about 0.3%, while the error obtained with SMR2 is 0.03%, which is equivalent to a gain of 95% in accuracy. For ω_{19}, the gain in accuracy is about 75% on the standard deviation estimation between SMR1 (error is 16%) and SMR2 (error is 4%). Regarding their PF, it can be noticed that they are higher than 0.5. Fig. 18 illustrates the number of random eigenvalues

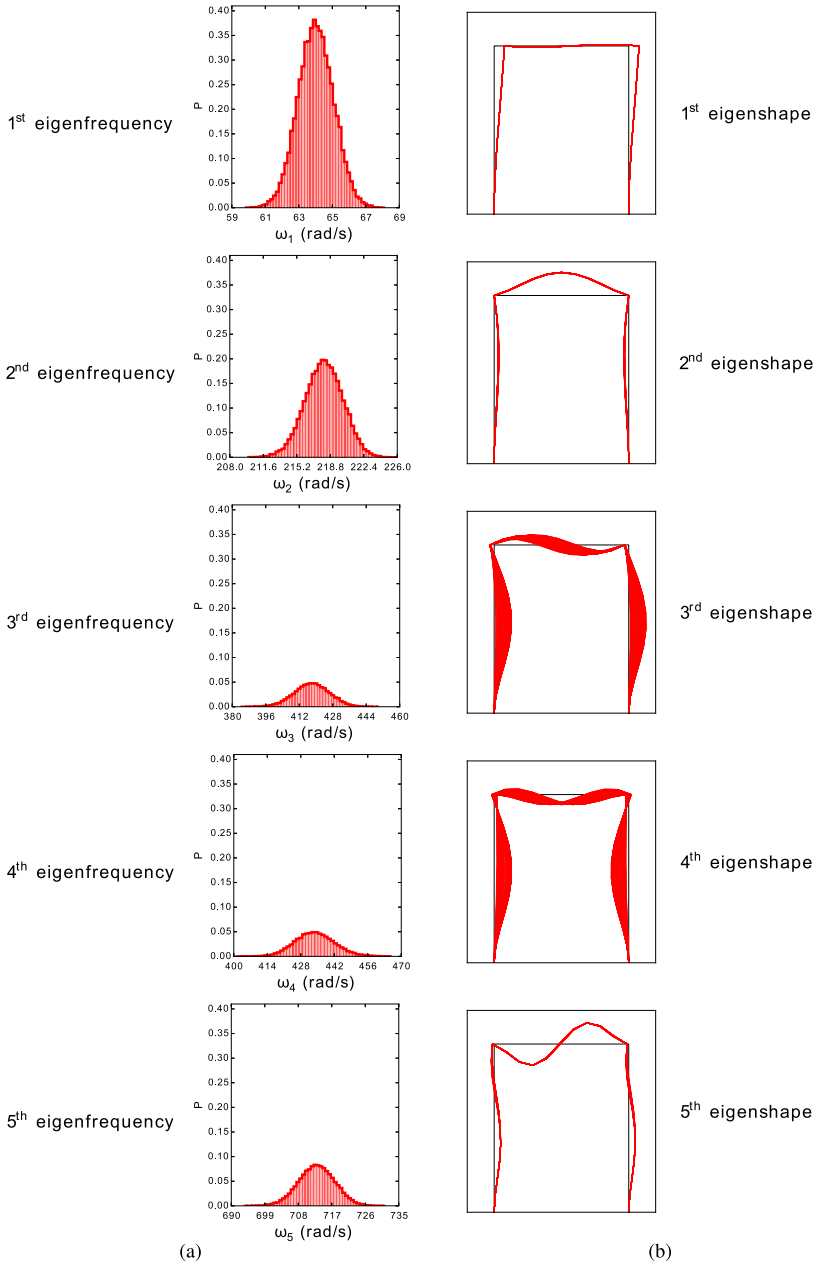

Fig. 12. Marginal density of the first five random frequencies (a) and the corresponding eigenshapes (b).

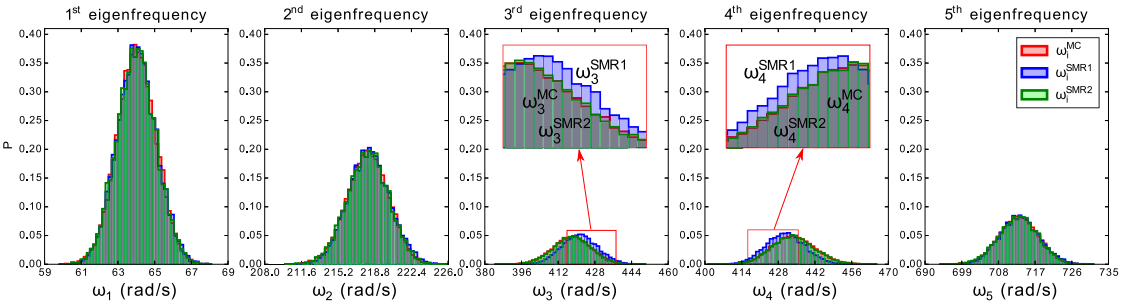

Fig. 13. Marginal density functions of the first five eigenfrequencies estimated with SMR1 and SMR2.

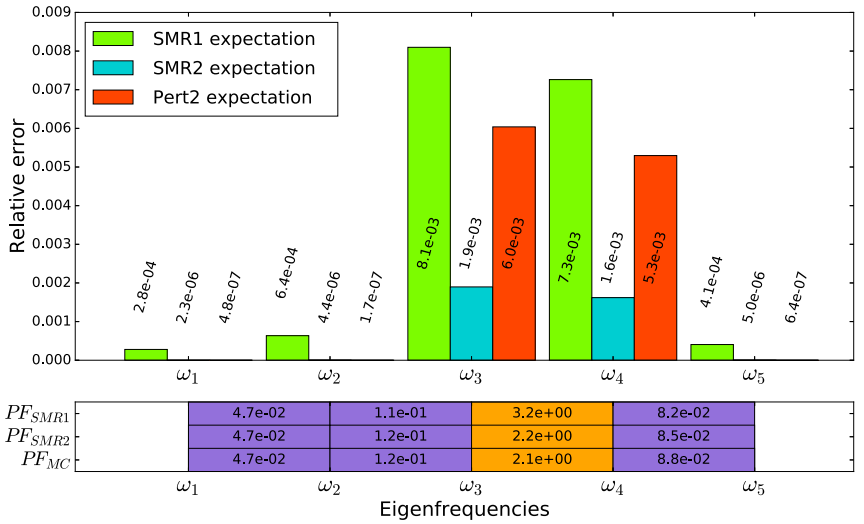

Fig. 14. Relative error of the expectation estimated with SMR1, SMR2 and the second-order perturbation method.

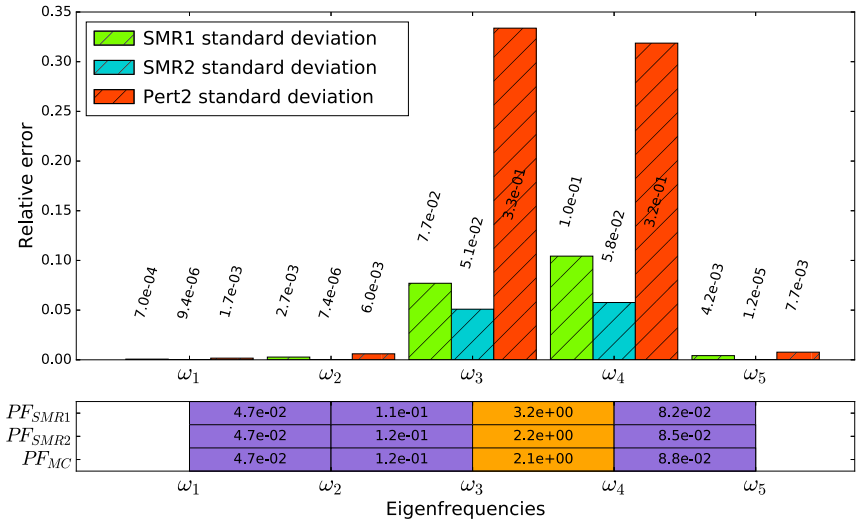

Fig. 15. Relative error of the standard deviation estimated with SMR1, SMR2 and the second-order perturbation method.

considered to be close depending on the limit value of PF. For a limit value $PF = 1$, there are 13 random eigenvalues identified to be close where SMR1 is not sufficient to estimate their first moments. For a limit value PF = 0.5, there are 16 close random eigenvalues, including ω_6 and ω_{19}. This illustrates the importance of the choice of the PF limit value criterion.

- For the 10th–11th eigenfrequencies, Figs. 16 and 17 show a difference between the indication of the proximity factor computed with SMR1 and the two other ones. This is because the three values are close to the limit value, but two are less than the limit, while the third one is slightly over. The proximity factor computed with SMR1 indicates that one needs to refine the method to get a more accurate result, while the reference proximity factor would have validated a less accurate estimation of the random eigenvalue. This particular case could be an advantage as well as a disadvantage, depending on the designer's point of view. The estimation accuracy is increased because the method used for this random eigenvalue will be refined. Nevertheless, it implies an additional computational cost for a low gain in accuracy. The criterion to choose if the method needs to be refined is an "all-or-nothing" criterion, while the proximity of two random eigenvalues is a concept more "fuzzy". Particular attention should be paid to PF values close to the limit value depending on the designer's objectives.
- For the case of the 23rd–24th eigenvalues, the two first moments estimations are not accurate either with SMR1 or with SMR2. This can be explained by the closeness of this couple of random eigenvalues. Indeed, the value of the corresponding proximity factor is far above the limit value PF = 1. The assumptions of the SMR1 and SMR2 methods are no longer valid, and the variability of the random eigenvectors is not well modeled. For this couple of random

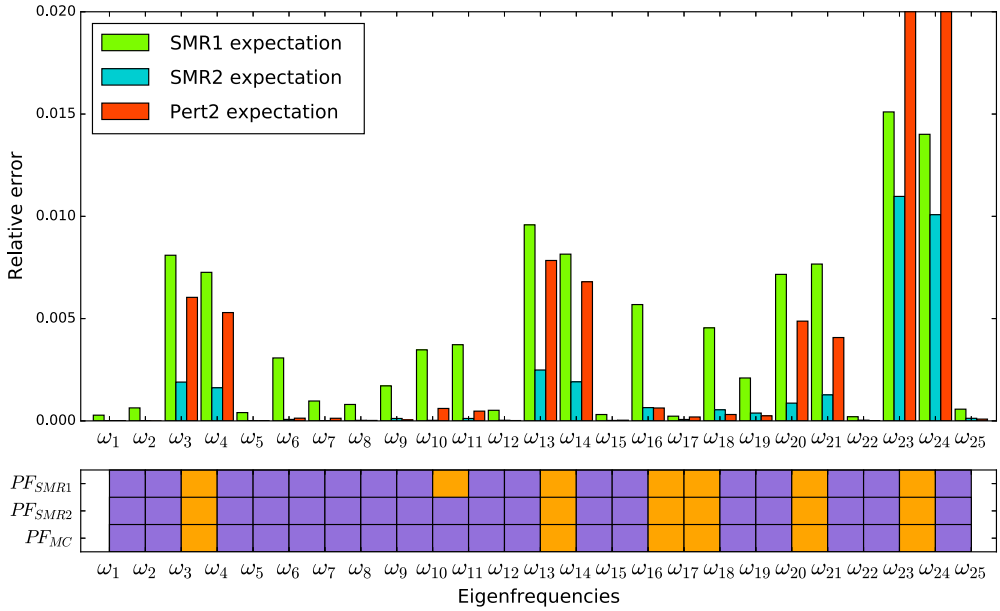

Fig. 16. Relative error in the estimation of the expectation for the first 25 random eigenfrequencies.

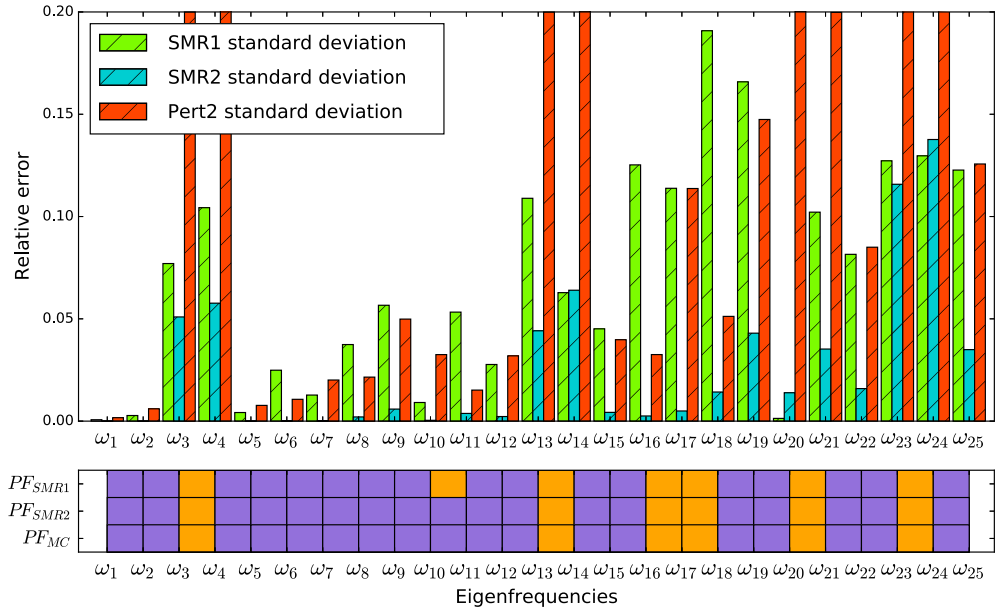

Fig. 17. Relative error in the estimation of the standard deviation for the first 25 random eigenfrequencies.

eigenvalues, it appears appropriate to estimate their corresponding random eigenvectors through a polynomial chaos expansion, for example [14].

6. Application to an industrial structure: the Ariane 5 payload adapter

This section presents the application of the SMR approach on an industrial structure corresponding to the Ariane 5 payload adapter. This is the occasion to apply the SMR approach coupled with a commercial finite element software. Ariane 5 is a heavy-lift launcher able to carry up to two loads to geostationary transfer orbit. Payloads are located under the fairing and positioned one under the other. Each payload is clamped on a frame named Payload Adapter System (PAS), which ensures an interface with the launcher. Fig. 19 presents the Ariane 5 launcher and one kind of PAS. Different kinds

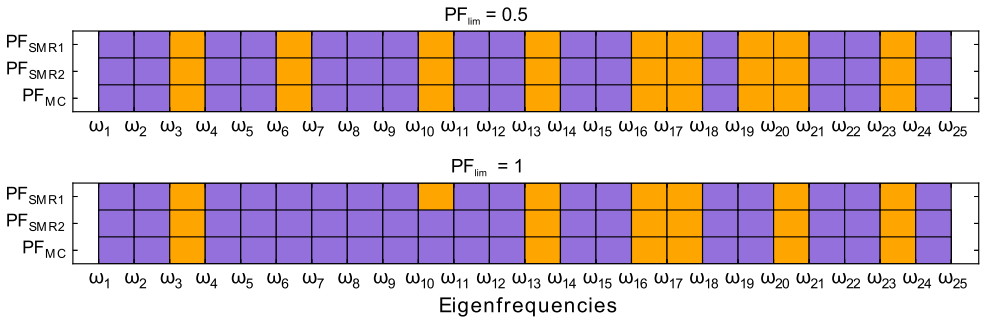

Fig. 18. Impact of the limit value of PF on the number of eigenvalues to be refined.

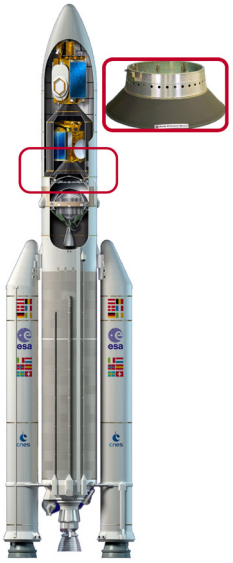

Fig. 19. Ariane 5 launcher and one of its payload adapter systems [55].

of PAS are available depending on the mission's profile. For the purpose of this work, we have chosen to study the PAS 1666MVS [55].

6.1. System modeling

The PAS 1666MVS consists of a conical structure with an upper interface compatible with the spacecraft and a bottom bolted interface compatible with the launcher. The lower cone of the PAS 1666MVS, as shown in Fig. 20a, is made of composite material. For the purpose of the SMR application case, it is assumed that the material is carbon epoxy composite with an isotropic homogenized Young modulus of expected value $\overline{Y}_{\text{Composite}} = 350000$ MPa. The Poisson ratio is 0.28 and the density is 1590 kg·m^{-3}. The upper cone is a monolithic aluminum part with a Young modulus of expected value $\overline{Y}_{\text{Alu}} = 70000$ MPa, a Poisson ratio of 0.3, and a density of 2800 kg·m^{-3}. An intermediate aluminum ring is included as a structure element of the lower composite cone. The bolted interface of the lower composite cone is made with another aluminum ring.

In a first approach, we assume that the Young moduli of the two different materials are independent random variables with Gamma distribution. Their expectation and coefficient of variation are respectively $\mathrm{E}[Y_{\text{Composite}}] = \overline{Y}_{\text{Composite}} = 350000$ MPa, $\mathrm{E}[Y_{\text{Alu}}] = \overline{Y}_{\text{Alu}} = 70000$ MPa, $\delta[Y_{\text{Composite}}] = \delta[Y_{\text{Alu}}] = 0.20$.

The PAS is axisymmetric, all the eigenmodes of the structure are then double eigenmodes. The framework of this paper is limited to the case of simple eigenmodes more or less close to each other. The SMR approach could be adapted to the case of multiple eigenmodes, but it is beyond the scope of this paper. To make the PAS test case dissymmetric, we propose to apply asymmetrical boundary conditions: PAS 1666MVS is clamped with the launcher through 72 regularly spaced bolted joints, and some angular portions of the bolted interface have been chosen unclamped. This is equivalent to a bound fault due to a link failure or an improper assembly. The requirement on the clamped solution enables us to obtain at least ten simple modes. A preliminary study has raised that the PAS with a single unclamped portion of $\pi/6$ rad has seven well-identified simples modes. To obtain at least ten simples modes, the selected configuration has three free portions: two small portions

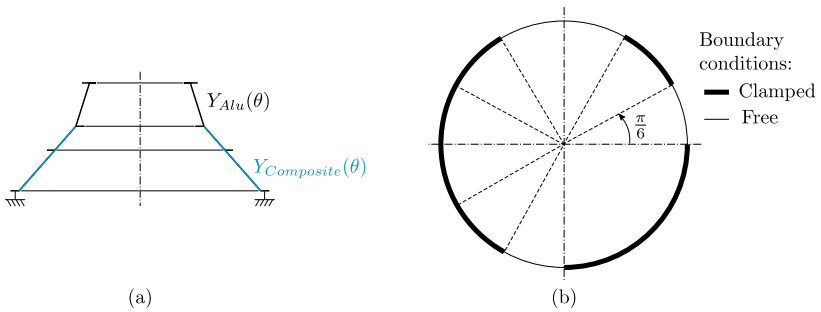

Fig. 20. Definition of the Ariane 5 Payload Adapter PAS 1666MVS. (a) Section of the PAS 1666MVS. (b) Definition of the clamped boundary conditions of the lower cone.

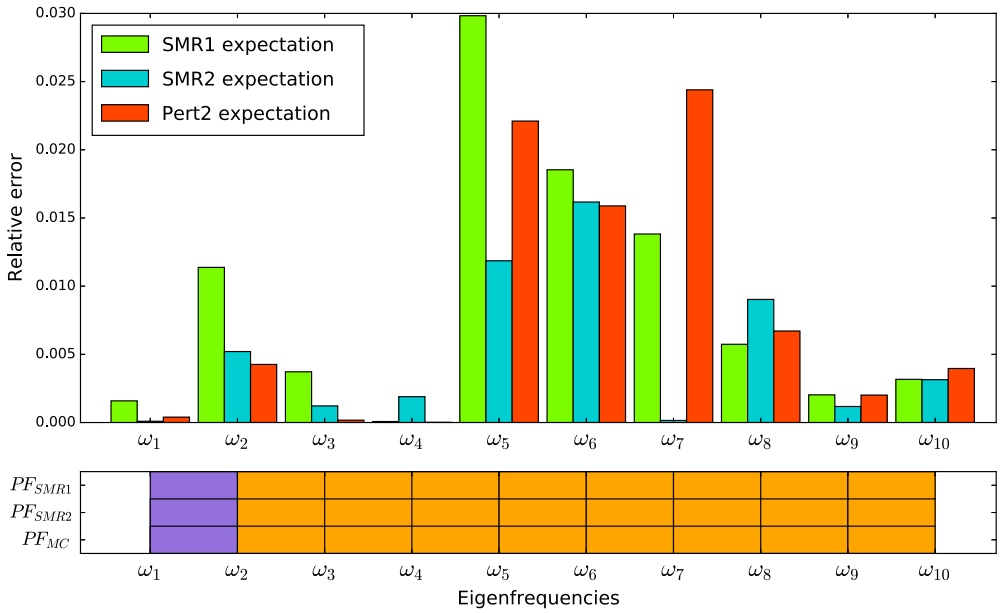

Fig. 21. Relative error of the expectation estimation of the PAS first 10 random eigenfrequencies.

of $\pi/6$ rad spaced with $\pi/2$ rad and a large portion of $\pi/3$ rad at $\pi/6$ rad from one of the small portions as defined in Fig. 20b. With this configuration, the first deterministic multiple mode is the twelfth one.

The finite element analysis of the PAS was achieved with the commercial software MSC Nastran. Shell elements have been used, and to avoid extreme computational time, the model is limited to 20000 degrees of freedom. A Monte Carlo simulation with 10000 samples allows us to compute the *pdf* of the first ten random eigenvalues of the PAS. It constitutes the reference framework to compare the results from the SMR method. This simulation has been performed on a quad-core computer Intel® Xeon® CPU E5507 − 2.27 GHz and 16 Gb DDR3-1066. It takes about 16 h.

6.2. Numerical results

The first ten random eigenvalues of the PAS are computed with SMR1, SMR2 and the second-order perturbation method. Figs. 21 and 22 show the relative errors of the two first statistical moments. The table below the error diagrams presents the proximity factor computed with SMR1, SMR2 and the reference from the Monte Carlo simulation.

Using only the SMR first refinement level, the expectation and the standard deviation of the first ten random eigenvalues of the PAS are estimated respectively with a maximum error of 3.0% and 12%. With the same computer as for the Monte Carlo simulation, this estimation is performed within a minute. The SMR second refinement level allows us to reduce the expectation and standard deviation maximum errors, respectively, to 1.6% and 9.2%. The computation of the first ten random eigenvalues with SMR2 takes less than 18 min. It can be noticed that the second-order perturbation method is again less accurate than SMR2 to estimate the standard deviation. Although the estimation of the expectation obtained with SMR2 is not always better than the estimation obtained with the second-order perturbation method, the relative error on the expectation estimation remains very satisfying (lower than 1.6% in any case), which does not contradict the use of SMR2.

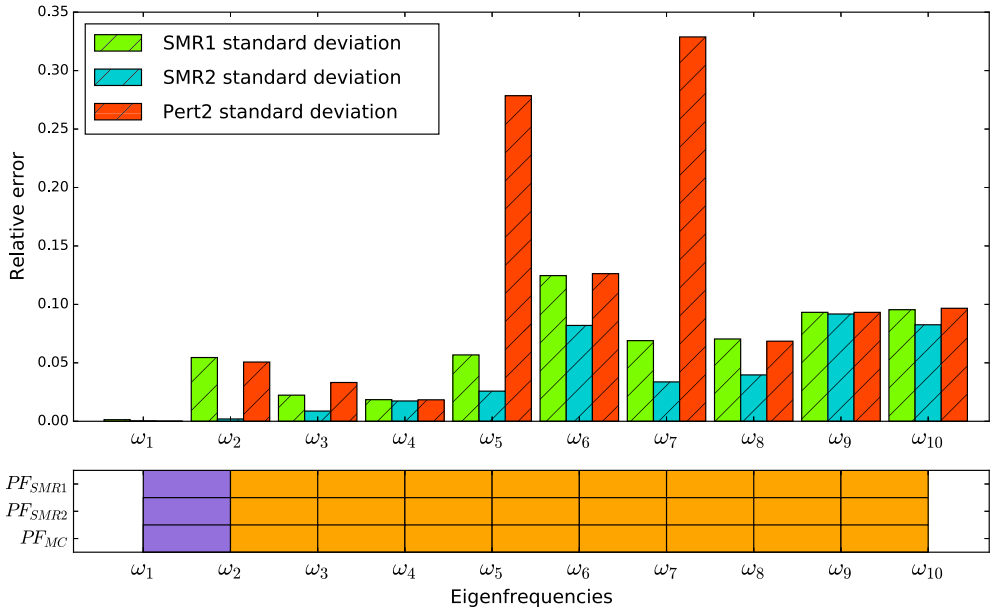

Fig. 22. Relative error of the standard deviation estimation of the PAS first 10 random eigenfrequencies.

This can be explained by the variability of the input parameters ($\delta = 0.20$). Indeed, the validity domain of the perturbation method is known to be bounded by coefficient of variation less than 20%.

The SMR approach recommends using the SMR second refinement level only when it is necessary. For this test case, the proximity factor suggests refining the method for almost all the random eigenvalues. Nevertheless, for the eigenfrequencies ω_3, ω_4 and ω_8 this refinement seems to be unnecessary. The proximity factor raises then some false-positive that does not ensure an optimized computational time. Inspired by the work of Perkins and Mote [21] and that of Du Bois [23], a way to overcome this issue could be to improve the proximity factor by taking into account the curvature of the reference response surface to identify when the response surface is sufficiently "plane" to be approximated with SMR1.

7. Conclusion

A non-intrusive approach to estimate the first two statistical moments of the random eigenvalues of a structure is presented. Referred to as SMR for Stochastic Model Reduction approach, it requires only a single deterministic finite element computation. This approach is based on the assumption that, in the vicinity of a given natural eigenfrequency, the dynamical behavior of a system is mainly characterized by the modal property of the considered eigenfrequency if all other eigenfrequencies are well separated. This leads one to assume the eigenvectors of the problem to be deterministic in the first approximation. This assumption is no longer valid when eigenvalues become closely spaced. In this case, the system becomes more coupled. So it is proposed to refine the method by considering the eigenvectors' randomness through their first-order Taylor expansion. To decide when the method should be refined, an indicator referred to as Proximity Factor, based on the first two statistical moments, is proposed. Computationally free, the efficiency of this indicator relies on the choice of its limit value criterion.

A first case of a three-degrees-of-freedom system is used to validate the approach and to characterize the behavior of the proximity factor. This example highlights the criticality of the choice of the limit value of this indicator over which the method needs to be refined. In a second application case, a frame with random Young's moduli allows us to apply the SMR approach to a wide range of random eigenfrequencies. We illustrate the SMR basis assumption by plotting the random eigenshapes of the frame. The ability of the proximity factor to identify when the method needs to be refined is demonstrated, and the criticality of its limit-value criterion is discussed. Finally, the approach is applied on an industrial structure modeled with a commercial software: the Ariane 5 payload adapter. This illustrates the SMR efficiency in comparison with Monte Carlo simulation. The first two statistical moments of the PAS first ten random eigenfrequencies are accurately estimated with a computational time reduction from 16 h to 18 min (i.e. a time reduction of 98%).

We conclude that the SMR method is an efficient method due to its ratio accuracy/computational-time. The proximity factor is a key parameter of the method, allowing one to refine only when it is necessary. Particular attention should be paid to the choice of the proximity factor limit value depending on the tradeoff accuracy/computational-time imposed by the designer.

Future works will focus on the improvement of the proximity factor. Indeed, the proposed proximity factor may give rise to a false positive, which may increase the global computation time of the approach without any significant accuracy improvement. It could then be improved, for example, by taking into account non-statistical quantities such as the curvature of

the eigenvalues response surfaces or by considering the correlation between two eigenvalues [52]. For this second approach, the computation of the complete covariance matrix has to be considered, which can not be obtained currently with SMR1. In addition, comparison with classical distances used in statistics such as the Mahalanobis distance [50,51] will be achieved to study the performance of the proximity factor. As the computational gain of the SMR method is even greater for large degree-of-freedom systems, the method could then be applied to more complex examples from industrial structures. Of particular interest is the case of bolted assembly where the stiffness of each bolted joint would be considered as a random variable. Bolted joints involve nonlinear phenomena as friction or contact. Future works will also focus on the application of the SMR approach to these kinds of nonlinear problems.

Appendix A. Calculation of the eigenvalue derivatives

In this section, the method for computing the eigenvalue derivatives introduced by [20] is briefly remembered. $\lambda_k(\mathbf{p})$ and $\mathbf{\Phi}_k(\mathbf{p})$ are the kth eigenvalue and eigenvector of the general undamped eigenvalue problem:

$$\mathbf{H}_k(\mathbf{p})\mathbf{\Phi}_k(\mathbf{p}) = \mathbf{0} \tag{40}$$

where $\mathbf{H}_k(\mathbf{p}) = \mathbf{K}(\mathbf{p}) - \lambda_k(\mathbf{p})\mathbf{M}(\mathbf{p})$. $\mathbf{M}(\mathbf{p})$ and $\mathbf{K}(\mathbf{p})$ designate respectively the mass and the stiffness matrices. All quantities of this problem depend on parameters p_i that are regrouped in the $\mathbf{p}$ vector.

By premultiplying the previous equation by $\mathbf{\Phi}_k(\mathbf{p})^\top$, the following equation could be considered:

$$\mathbf{\Phi}_k(\mathbf{p})^\top \mathbf{H}_k(\mathbf{p})\mathbf{\Phi}_k(\mathbf{p}) = 0 \tag{41}$$

Differentiating Eq. (41) with respect to a parameters p_i leads to the following equation:

$$\underbrace{\frac{\partial \mathbf{\Phi}_k(\mathbf{p})^\top}{\partial p_i}\mathbf{H}_k(\mathbf{p})\mathbf{\Phi}_k(\mathbf{p})}_{E_1(\mathbf{p})} + \mathbf{\Phi}_k(\mathbf{p})^\top \frac{\partial \mathbf{H}_k(\mathbf{p})}{\partial p_i}\mathbf{\Phi}_k(\mathbf{p}) + \underbrace{\mathbf{\Phi}_k(\mathbf{p})^\top \mathbf{H}_k(\mathbf{p})\frac{\partial \mathbf{\Phi}_k(\mathbf{p})}{\partial p_i}}_{E_2(\mathbf{p})} = 0 \tag{42}$$

Due to Eq. (40) and the symmetric property of matrix $\mathbf{H}_k(\mathbf{p})$, terms $E_1(\mathbf{p})$ and $E_2(\mathbf{p})$ vanish. So Eq. (42) becomes:

$$\mathbf{\Phi}_k(\mathbf{p})^\top \frac{\partial \mathbf{H}_k(\mathbf{p})}{\partial p_i}\mathbf{\Phi}_k(\mathbf{p}) = 0 \tag{43}$$

In addition, the calculation of $\dfrac{\partial \mathbf{H}_k(\mathbf{p})}{\partial p_i}$ using the derivatives of $\mathbf{M}(\mathbf{p})$ and $\mathbf{K}(\mathbf{p})$ with respect to p_i leads to

$$\frac{\partial \mathbf{H}_k(\mathbf{p})}{\partial p_i} = \frac{\partial \mathbf{K}(\mathbf{p})}{\partial p_i} - \lambda_k(\mathbf{p})\frac{\partial \mathbf{M}(\mathbf{p})}{\partial p_i} - \frac{\partial \lambda_k(\mathbf{p})}{\partial p_i}\mathbf{M}(\mathbf{p}) \tag{44}$$

If the eigenvectors are assumed to be $\mathbf{M}$-orthogonal ($\mathbf{\Phi}_k(\mathbf{p})^\top \mathbf{M}\mathbf{\Phi}_k(\mathbf{p}) = 1$), the use of Eqs. (42) and (44) leads to the derivatives with respect to p_i of the kth eigenvalue:

$$\frac{\partial \lambda_k(\mathbf{p})}{\partial p_i} = \mathbf{\Phi}_k(\mathbf{p})^\top \left[\frac{\partial \mathbf{K}(\mathbf{p})}{\partial p_i} - \lambda_k(\mathbf{p})\frac{\partial \mathbf{M}(\mathbf{p})}{\partial p_i}\right]\mathbf{\Phi}_k(\mathbf{p}) \tag{45}$$

References

[1] C. Blanzé, L. Champaney, A computational strategy for the random response of assemblies of structures, Int. J. Solids Struct. 41 (2004) 6383–6405.
[2] C. Blanzé, P. Rouch, Analysis of structures with stochastic interfaces in the medium-frequency range, J. Comput. Acoust. 13 (04) (2005) 711–729.
[3] M. Shinozuka, C.J. Astill, Random eigenvalue problems in structural analysis, AIAA J. 10 (4) (1972) 456–462.
[4] C.A. Schenk, G.I. Schüller, Uncertainty Assessment of Large Finite Element Systems, Lecture Notes in Applied and Computational Mechanics, vol. 24, Springer, Berlin, Heidelberg, 2005, pp. 59–61, chapter 9.
[5] C. Germoso, J.V. Aguado, A. Fraile, E. Alarcon, F. Chinesta, Efficient PGD-based dynamic calculation of non-linear soil behavior, C. R., Méc. 344 (1) (2016) 24–41.
[6] B. Sudret, A. Der Kiureghian, Stochastic Finite Element Methods and Reliability: A State-of-the-Art Report, Technical Report, 2000.
[7] J.D. Collins, W.T. Thomson, The eigenvalue problem for structural systems with statistical properties, AIAA J. 7 (4) (April 1969) 642–648.
[8] S. Adhikari, M.I. Friswell, Random matrix eigenvalue problems in structural dynamics, Int. J. Numer. Methods Eng. 69 (3) (2007) 562–591.
[9] P.B. Nair, A.J. Keane, An approximate solution scheme for the algebraic random eigenvalue problem, J. Sound Vib. 260 (1) (2003) 45–65.
[10] R. Ghanem, P.D. Spanos, Polynomial chaos in stochastic finite elements, J. Appl. Mech. 57 (1) (1990) 197–202.
[11] N. Wiener, The homogeneous chaos, Amer. J. Math. 60 (4) (1938) 897–936.
[12] R.G. Ghanem, P.D. Spanos, Stochastic Finite Elements: A Spectral Approach, revised edition, New York, Dover, 2003.
[13] D. Xiu, G.E. Karniadakis, Modeling uncertainty in flow simulations via generalized polynomial chaos, J. Comput. Phys. 187 (1) (2003) 137–167.
[14] R. Ghanem, D. Ghosh, Efficient characterization of the random eigenvalue problem in a polynomial chaos decomposition, Int. J. Numer. Methods Eng. 72 (4) (2007) 486–504.
[15] R. Ghanem, D. Ghosh, Eigenvalue analysis of a random frame, in: EURODYN2002, Munich, Germany, 2–5 September, 2002, p. 341.
[16] D. Ghosh, R. Ghanem, C. Petit, Stochastic buckling of a joined wing, in: Stochastic Dynamics Conference, Hangzhou, China, 26–28 May, 2003.

[17] B. Pascual, S. Adhikari, Hybrid perturbation-polynomial chaos approaches to the random algebraic eigenvalue problem, Comput. Methods Appl. Mech. Eng. 217 (2012) 153–167.
[18] Y. Karim, C. Blanzé, Vibration reduction by piezo-electric shunt: taking into account of uncertainties by non-intrusive methods, in: Proceedings of Uncertainties 2014, Rouen, France, June 23–27, 2014.
[19] Y. Karim, Caractérisation robuste de liaisons amortissantes avec dispositifs piezo-électriques pour la réduction de vibrations de structures, PhD Thesis, Conservatoire national des arts et métiers – CNAM, December 2013.
[20] R.L. Fox, M.P. Kapoor, Rates of change of eigenvalues and eigenvectors, AIAA J. 6 (12) (1968) 2426–2429.
[21] N.C. Perkins, C.D. Mote, Comments on curve veering in eigenvalue problems, J. Sound Vib. 106 (3) (1986) 451–463.
[22] E. Balmes, High modal density, curve veering, localization – a different perspective on the structural response, J. Sound Vib. 161 (1993) 358–363.
[23] J.L. Du Bois, S. Adhikari, N.A.J. Lieven, On the quantification of eigenvalue curve veering: a veering index, J. Appl. Mech. 78 (4) (2011), pp. 041007-1–041007-8.
[24] I. Hirai, M. Kashiwaki, Derivatives of eigenvectors of locally modified structures, Int. J. Numer. Methods Eng. 11 (11) (1977) 1769–1773.
[25] S. Garg, Derivatives of eigensolutions for a general matrix, AIAA J. 11 (8) (1973) 1191–1194.
[26] C.S. Rudisill, Y.-Y. Chu, Numerical methods for evaluating the derivatives of eigenvalues and eigenvectors, AIAA J. 13 (6) (1975) 834–837.
[27] L.C. Rogers, Derivatives of eigenvalues and eigenvectors, AIAA J. 8 (5) (1970) 943–944.
[28] K.F. Alvin, Efficient computation of eigenvector sensitivities for structural dynamics, AIAA J. 35 (11) (1997) 1760–1766.
[29] R.M. Lin, Z. Wang, M.K. Lim, A practical algorithm for the efficient computation of eigenvector sensitivities, Comput. Methods Appl. Mech. Eng. 130 (3–4) (1996) 355–367.
[30] R.B. Nelson, Simplified calculation of eigenvector derivatives, AIAA J. 14 (9) (1976) 1201–1205.
[31] M.I. Friswell, Calculation of second and higher order eigenvector derivatives, J. Guid. Control Dyn. 18 (4) (1995) 919–921.
[32] M.I. Friswell, The derivatives of repeated eigenvalues and their associated eigenvectors, J. Vib. Acoust. 118 (3) (1996) 390–397.
[33] I.U. Ojalvo, Efficient computation of mode-shape derivatives for large dynamic systems, AIAA J. 25 (10) (1987) 1386–1390.
[34] W.C. Mills-Curran, Calculation of eigenvector derivatives for structures with repeated eigenvalues, AIAA J. 26 (7) (1988) 867–871.
[35] W.C. Mills-Curran, Comment on “Eigenvector derivatives with repeated eigenvalues”, AIAA J. 28 (10) (1990), 1846–1846.
[36] R. Lane Dailey, Eigenvector derivatives with repeated eigenvalues, AIAA J. 27 (4) (April 1989) 486–491.
[37] T.-Y. Chen, Design sensitivity analysis for repeated eigenvalues in structural design, AIAA J. 31 (12) (1993) 2347–2350.
[38] I.-W. Lee, G.-H. Jung, An efficient algebraic method for the computation of natural frequency and mode shape sensitivities – part I, distinct natural frequencies, Comput. Struct. 62 (3) (1997) 429–435.
[39] A.D. Belegundu, B.G. Yoon, Iterative methods for design sensitivity analysis, AIAA J. 26 (11) (1988) 1413–1415.
[40] A.L. Andrew, R.C.E. Tan, Computation of mixed partial derivatives of eigenvalues and eigenvectors by simultaneous iteration, Commun. Numer. Methods Eng. 15 (9) (1999) 641–649.
[41] M.S. Jankovic, Exact nth derivatives of eigenvalues and eigenvectors, J. Guid. Control Dyn. 17 (1) (1994) 136–144.
[42] N. Olhoff, E. Lund, A.P. Seyranian, Sensitivity analysis and optimization of multiple eigenvalues in structural design problems, Struct. Optim. 8 (4) (1994) 207–227.
[43] E. Lund, N. Olhoff, Shape design sensitivity analysis of eigenvalues using “exact” numerical differentiation of finite element matrices, Struct. Optim. 8 (1) (1994) 52–59.
[44] H.C. Mateus, H.C. Rodrigues, C.M. Mota Soares, C.A. Mota Soares, Sensitivity analysis and optimization of thin laminated structures with a nonsmooth eigenvalue based criterion, Struct. Optim. 14 (4) (1997) 219–224.
[45] I.-W. Lee, D.-O. Kim, G.-H. Jung, Natural frequency and mode shape sensitivities of damped systems: part I, distinct natural frequencies, J. Sound Vib. 223 (3) (1999) 399–412.
[46] I.-W. Lee, D.-O. Kim, G.-H. Jung, Natural frequency and mode shape sensitivities of damped systems: part II, multiple natural frequencies, J. Sound Vib. 223 (3) (1999) 413–424.
[47] Electricité de France, Finite element code_aster, analysis of structures and thermomechanics for studies and research, 1989–2017, open source on www.code-aster.org.
[48] R.H. Plaut, K. Huseyin, Derivatives of eigenvalues and eigenvectors in non-self-adjoint systems, AIAA J. 11 (2) (February 1973) 250–251.
[49] C.S. Manohar, A.J. Keane, Statistics of energy flows in spring-coupled one-dimensional subsystems, Philos. Trans. R. Soc., Math. Phys. Eng. Sci. 346 (1681) (1994) 525–542.
[50] P.C. Mahalanobis, On the generalised distance in statistics, Proc. Natl. Inst. Sci. India, a Phys. Sci. 2 (1) (1936) 49–55.
[51] C. Archambeau, F. Vrins, M. Verleysen, Flexible and robust Bayesian classification by finite mixture models, in: Proceedings of 12th European Symposium on Artificial Neural Networks, 2004, pp. 75–80, ESANN 2004, Bruges, Belgium, April 28–30, 2004.
[52] S. Adhikari, Joint statistics of natural frequencies of stochastic dynamic systems, Comput. Mech. 40 (4) (Sep. 2007) 739–752.
[53] C. Soize, Stochastic modeling of uncertainties in computational structural dynamics – recent theoretical advances, J. Sound Vib. 332 (10) (2013) 2379–2395.
[54] E.T. Jaynes, Information theory and statistical mechanics, Phys. Rev. 106 (1957) 620–630.
[55] Arianespace S.A. Ariane 5, User’s Manual, Arianespace S.A., Issue 5, Revision 1 edition, July 2011.